Complementary Quantitative Proteomics Reveals that Transcription Factor AP-4 Mediates E-box-dependent Complex Formation for Transcriptional Repression of *HDM2**⑤

Wei-Chi Ku‡§, Sung-Kay Chiu¶, Yi-Ju Chen‖, Hsin-Hung Huang‖, Wen-Guey Wu‡§, and Yu-Ju Chen‡**‡‡§§

Transcription factor activating enhancer-binding protein 4 (AP-4) is a basic helix-loop-helix protein that binds to E-box elements. AP-4 has received increasing attention for its regulatory role in cell growth and development, including transcriptional repression of the human homolog of murine double minute 2 (HDM2), an important oncoprotein controlling cell growth and survival, by an unknown mechanism. Here we demonstrate that AP-4 binds to an E-box located in the *HDM2*-P2 promoter and represses *HDM2* transcription in a p53-independent manner. Incremental truncations of AP-4 revealed that the C-terminal Gln/Pro-rich domain was essential for transcriptional repression of *HDM2*. To further delineate the molecular mechanism(s) of AP-4 transcriptional control and its potential implications, we used DNA-affinity purification followed by complementary quantitative proteomics, cICAT and iTRAQ labeling methods, to identify a previously unknown E-box-bound AP-4 protein complex containing 75 putative components. The two labeling methods complementarily quantified differentially AP-4-enriched proteins, including the most significant recruitment of DNA damage response proteins, followed by transcription factors, transcriptional repressors/corepressors, and histone-modifying proteins. Specific interaction of AP-4 with CCCTC binding factor, stimulatory protein 1, and histone deacetylase 1 (an AP-4 corepressor) was validated using AP-4 truncation mutants. Importantly, inclusion of trichostatin A did not alleviate AP-4-mediated repression of *HDM2* transcription, suggesting a previously unidentified histone deacetylase-independent repression mechanism. In contrast, the complementary quantitative proteomics study suggested that transcription repression occurs via coordination of AP-4 with other transcription factors, histone methyltransferases, and/or a nucleosome remodeling SWI·SNF complex. In addition to previously known functions of AP-4, our data suggest that AP-4 participates in a transcriptional-regulating complex at the *HDM2*-P2 promoter in response to DNA damage. *Molecular & Cellular Proteomics 8: 2034–2050, 2009.*

Transcription factor activating enhancer binding-protein 4 (AP-4)[1] is a ubiquitously expressed transcription factor belonging to the basic helix-loop-helix (bHLH) superfamily and binds to the consensus E-box sequence 5′-CAGCTG-3′ (1, 2). It was first identified as a cellular factor that binds to the simian virus 40 enhancer sequence and interacts synergistically with AP-1 to increase viral late gene transcription *in vitro*

[1] The abbreviations used are: AP-4, activating enhancer-binding protein 4; APEX1, DNA-(apurinic or apyrimidinic site) lyase; bHLH, basic-helix-loop-helix; ChIP, chromatin immunoprecipitation; cICAT, cleavable isotope-coded affinity tag; CLOCK, circadian locomotor output cycles protein kaput; CTBP1, C-terminal-binding protein 1; FA, formic acid; HDM2, human homolog of murine double minute 2; *HDM2*-P2, *HDM2* promoter P2; HIV-1, human immunodeficiency virus type 1; HMG, high mobility group protein; iTRAQ, isobaric tags for relative and absolute quantitation; LC-ESI-MS/MS, liquid chromatography electrospray ionization tandem mass spectrometry; LR, leucine repeat; MU, mutant; NFAT, nuclear factor of activated T cells; NRSF, neuron restrictive silencer factor, also known as REST; p53 RE, p53 responsive element; *PAHX-AP1*, phytanoyl-CoA α-hydroxylase-associated protein 1; PARP2, poly-[ADP-ribose] polymerase 2; PCNA, proliferating cell nuclear antigen; POLE2, DNA polymerase epsilon subunit 2; Q/P-rich, glutamine/proline-rich; SCX, strong cation exchange; SWI·SNF, SWItch/Sucrose NonFermentable; SMARC, SWI·SNF-related matrix-associated actin-dependent regulator of chromatin; SP1, stimulatory protein 1; TBP, TATA-binding protein; TERF2, telomeric repeat-binding protein 2; TOF, time-of-flight; TSA, trichostatin A; TTBS, tris-tween buffered saline; USF2, upstream stimulatory factor 2; WT, wild-type; TEMED, *N,N,N′,N′*-tetramethylenediamine; TEABC, triethylammonium bicarbonate; TCEP, Tris (2-carboxyethyl)-phosphine.

(2). Since its discovery, AP-4 has become recognized for its important role in modulation of cellular functions via regulation of genes involved in viral production (2–6), cell growth and survival (7–12), immune response (13–15), and angiogenesis (16). Sequence analysis has revealed that, unlike other bHLH proteins, AP-4 contains several protein-protein-interacting domains, including a bHLH domain and two distinct leucine repeat (LR) domains (1). The activity of many proteins is controlled by their cooperation and interplay within protein complexes. Likewise, the multiple protein-protein interaction domains within AP-4 suggest that it may achieve gene-specific transcriptional regulation by dynamic interaction with a wide variety of transcription factors or cofactors (1, 17). For example, AP-4 represses neuron-specific *PAHX-AP1* transcription by forming a protein complex with the transcription corepressor geminin (18), and it activates the transcriptional activity of dopamine β-hydroxylase by interacting with GATA-3 and SP1 (19).

The oncoprotein, human homolog of murine double minute 2 (HDM2), has been recognized as an important molecule in regulating cell proliferation and DNA damage response (20). It is well established that HDM2 and p53 form a negative auto-regulatory feedback loop, in which p53 activates *HDM2* transcription, and HDM2 acts as a negative regulator of p53 (21–23). However, there is considerable evidence suggesting that HDM2 has tumorigenic properties independent of p53, implicating HDM2 as a potential target for cancer therapy (20). Inhibition of HDM2 has been reported to result in tumorigenic inhibition and chemotherapeutic sensitization in various human cancers (24). A recent study has shown that HDM2 activity was down-regulated upon AP-4 overexpression, possibly via transcriptional repression (25). However, how AP-4 regulates *HDM2* transcription remains elusive because AP-4 response element has not been identified in the *HDM2* promoter (25). On the other hand, AP-4 has been shown to repress gene transcription by forming protein complexes with transcription repressors (18); therefore implying the possibility that it may rely on a similar mechanism to repress *HDM2* transcription. To uncover the repressive mechanism at the molecular level, identification of protein complexes associated with AP-4 at the *HDM2*-P2 promoter is necessary. Elucidation of the mechanism of *HDM2* transcriptional repression by AP-4 may also lead to a better understanding of the regulatory network between AP-4 and HDM2 as well as the potential role of AP-4 as a target for cancer therapy.

Despite the technological advances of mass spectrometry for protein characterization, identification of specific DNA-bound protein complexes has proven to be a challenge using the classical single-step DNA-affinity isolation (26). Transcription factors that bind to specific promoters only account for <0.01% of the total cellular protein (27). Thus, the low abundance of transcription factors necessitates purification from nuclear extracts prepared from a large number of cultured cells to achieve the 10,000- to 100,000-fold enrichment,

which is required to obtain sufficient amounts of protein for further chemical and functional analyses (28). However, non-specific protein-DNA interactions inevitably arise from the binding of positively charged proteins to the DNA sequence of interest and mask identification of the sequence-specific components of DNA-binding protein complexes. Quantitative proteomics using stable isotope labeling methods, such as ICAT (29) or iTRAQ (30), in combination with single-step DNA-affinity purification can circumvent these problems via quantitative comparison of the extent of enrichment between wild-type (WT) and mutant (MU) DNA sequence-bound proteins. The comparison of isotopically labeled protein abundance enriched during DNA pull-down experiments allows discrimination of specific DNA-protein complex components from contaminating proteins originating from the purification background (26). These isotopic labeling strategies have been successfully used to study the dynamics of transcriptional complex formation during erythroid differentiation (31), to identify the dynamic components of the large RNA polymerase II pre-initiation complex (32, 33) as well as the TATA-binding protein (TBP) transcription complex (34), to identify the transcription factor Six4 bound to the muscle creatine kinase enhancer (35), and to identify transcription factor MAZ as a regulator of muscle-specific genes (36). Therefore, we utilized quantitative proteomics to facilitate identification of potential AP-4 complexes at the *HDM2* promoter.

To explore the potential role of AP-4 in regulating *HDM2* transcription, we investigated AP-4-mediated repression of *HDM2* transcription by examining binding of AP-4 and associated proteins to the *HDM2* promoter. First, we showed that AP-4 bound to a previously uncharacterized E-box in *HDM2*-P2 promoter and demonstrated that AP-4 repressed *HDM2* transcription in a dose-dependent and p53-independent manner. Next, we characterized AP-4 complex bound to the *HDM2*-P2 promoter using single-step DNA-affinity purification in combination with complementary quantitative proteomics using cICAT and iTRAQ labeling. The two complementary methods allowed quantitative identification of many transcriptional repressors/corepressors, histone-modifying enzymes, and, in particular, several DNA damage-response proteins in the AP-4 complex; proteins in the latter category suggest a potential function of AP-4 in the DNA damage response. Furthermore, Western blotting confirmed that cICAT- and iTRAQ-labeling methods identified distinct DNA-enriched AP-4-associated proteins, highlighting the importance of complementary quantitative proteomics for identifying protein complex components. Together with DNA pull-downs and luciferase assays using incremental truncations of AP-4, the quantitative proteomics approach allowed us to conclude that AP-4 represses *HDM2* transcription via an HDAC- and p53-independent mechanism and to identify many of the accessory proteins involved in AP-4-mediated repression.

EXPERIMENTAL PROCEDURES

Chemicals—Monomeric acrylamide/bisacrylamide solution (40%, 29:1) was purchased from Bio-Rad. Trypsin (modified, sequencing grade) was obtained from Promega (Madison, WI). The BCA and Bradford protein assay reagent kits were obtained from Pierce. SDS, Tris, urea, ammonium persulfate, iodoacetamide, and *N,N,N′,N′*-tetramethylenediamine (TEMED) were purchased from Amersham Biosciences. EDTA and methanol were purchased from Merck (Darmstadt, Germany). Bromphenol blue, β-mercaptoethanol, Tris (2-carboxyethyl)-phosphine hydrochloride (TCEP-HCl), triethylammonium bicarbonate (TEABC), ammonium bicarbonate (ABC), phosphate-buffered saline, potassium hydroxide (KOH), potassium chloride (KCl), poly(deoxyinosinic-deoxycytidylic) acid, glycerol, magnesium chloride hexahydrate, dithiothreitol, HEPES, imidazole, methyl methanethiosulfonate, Triton X-100, trifluoroacetic acid, trichostatin A (TSA), and high pressure liquid chromatography (HPLC)-grade ACN were purchased from Sigma-Aldrich. Formic acid (FA) and potassium dihydrogen phosphate (KH_2PO_4) were purchased from Riedel de Haen (Seelze, Germany). Water was purified using a Milli-Q® Ultrapure Water Purification System from Millipore (Billerica, MA). Nonidet P-40 was obtained from Calbiochem. Tris borate-EDTA (TBE) buffer was obtained from Amresco (Solon, OH).

Cell Lines—HCT116 p53$^{+/+}$ and HCT116 p53$^{-/-}$ cells lines, which were generous gifts from Professor Bert Vogelstein (Johns Hopkins University), were maintained at 37 °C in Dulbecco's modified Eagle's medium (HyClone, Logan, UT) supplemented with 10% heat-inactivated fetal bovine serum (Invitrogen) and antibiotic-antimycotic (Invitrogen), which contained a final concentration of 100 units/ml of penicillin (base), 100 μg/ml of streptomycin (base), and 0.25 μg/ml of amphotericin B.

Plasmids—To construct the AP-4 bacterial expression plasmid pTriEx-4-AP-4 encoding a His$_6$ tag at the N terminus, full-length AP-4 cDNA was amplified by reverse transcription (RT)-PCR from HeLa mRNA and cloned into the pTriEx^{TM}-4-neo plasmid (Novagen, Madison, WI).

To generate various plasmids expressing incremental truncations of AP-4 without any tag, including pcDNA-AP-4 (full-length), pcDNA-ΔN99 (residues 100–339), pcDNA-ΔN142 (residues 143–339), pcDNA-ΔN179 (residues 180–339), pcDNA-ΔC51 (residues 1–289), pcDNA-ΔC89 (residues 1–244), pcDNA-ΔC159 (residues 1–179), pcDNA-ΔC197 (residues 1–142), and pcDNA-ΔC239 (residues 1–99), various AP-4 cDNA fragments were amplified by PCR with appropriate oligonucleotide primers using pTriEx-4-AP-4 as the template. PCR products were subcloned into the pcDNA^{TM} 3.1/*myc*-His (−) A vector (Invitrogen). A stop codon (TGA) was included in all reverse PCR primers to exclude the vector-born C-terminal *myc* and His tags.

For the construction of various plasmids expressing incremental truncations of AP-4 encoding an N-terminal FLAG tag, pcDNA-AP-4 (full-length) and the truncation mutants described above were individually digested with EcoRI and HindIII restriction endonucleases (New England Biolabs, Beverly, MA). The restriction fragments were subcloned into the pCMV-Tag 2B expression plasmid (Stratagene, La Jolla, CA).

The luciferase reporter plasmid containing the *HDM2*-P2 promoter in pGL3-Basic (Promega), designated as hdm2luc01-WT, was constructed as described (37). To generate the reporter plasmid containing the mutant E-box located at −29 to −34 bp from the transcription start site (hdm2luc01-MU), hdm2luc01-WT plasmid was subjected to overlap extension PCR (38) using the mutagenic primers 5′-TCTC-*GAATTCG*GGGCTATTTAAACCATGC-3′ (forward) and 5′-GCCC*GAAT-TCG*AGACAAGTCAGGACTTA-3′ (reverse) (sequence mutations are underlined). All plasmid constructs described above were verified by DNA sequencing.

Antibodies—To generate in-house rabbit anti-AP-4, His-tagged AP-4 (His-AP-4) was first purified from inclusion bodies treated with 6 M urea following isopropyl 1-thio-β-D-galactopyranoside (IPTG) induction of *Escherichia coli* Tuner(DE3)pLacI (Novagen) cells transformed with pTriEx-4-AP-4 or by His-affinity chromatography using Talon^{TM} superflow resin (Clontech, Palo Alto, CA). His-AP-4 was refolded on-column, eluted with 100 mM imidazole, and further purified using a HiTrap^{TM} Heparin HP column (Amersham Biosciences). Rabbit polyclonal anti-AP-4 antibody was generated by IgMedica Biotech (Taipei, Taiwan) using 1 mg of purified His-AP-4 as antigen. The antibody was further purified using Protein G chromatography and dialyzed against phosphate-buffered saline containing 0.1% (v/v) Triton X-100.

Other antibodies including goat anti-AP-4 (SC-18593X), goat anti-CTBP1 (SC-5961), goat anti-actin (SC-1615), mouse anti-NFATc2 (SC-7296), mouse anti-APEX1 (SC-17774), mouse anti-USF2 (SC-81421), rabbit anti-PCNA (SC-7907), and rabbit anti-HMGB1 (SC-33199) were purchased from Santa Cruz Biotechnology (Santa Cruz, CA). Rabbit anti-CTCF (07–729), rabbit anti-SP1 (17–601), rabbit anti-histone H3 (06–755), rabbit anti-acetyl-histone H3 (09–599), mouse anti-HDAC1 (05–614), and mouse anti-HDAC2 (05–814) antibodies were purchased from Millipore. Mouse anti-p53 (OP43T) antibody was purchased from Calbiochem. Mouse anti-FLAG M2 antibody was purchased from Stratagene.

Electrophoretic Mobility Shift Assays (EMSA)—EMSA were performed using the LightShift Chemiluminescent EMSA kit (Pierce) following the manufacturer's procedure. Complementary double-stranded oligonucleotides corresponding to the −43 to −20 region of the *HDM2*-P2 promoter containing WT (sense strand: 5′-biotin-ACT-TGTCTC*CAGCTG*GGGGCTATTT-3′) or MU (sense strand: 5′-biotin-ACTTGTCTC*GAATTC*GGGCTATTT-3′) E-box sequences were prepared by Bio Basic Inc. (Ontario, Canada). For EMSA reactions, 10 μg of nuclear extract was incubated with 20 fmol of double-stranded biotin-labeled WT oligonucleotide in a 20-μl reaction containing 10 mM Tris (pH 7.5), 50 mM KCl, 1 mM dithiothreitol, 50 ng/μl poly(deoxyinosinic-deoxycytidylic) acid, 2.5% (v/v) glycerol, 0.05% (v/v) Nonidet P-40, and 1 mM MgCl$_2$ at room temperature for 20 min. For antibody super-shift experiments, 1 μg of normal goat serum or goat anti-AP-4 was added to the reactions and further incubated on ice for 30 min. Reactions were subjected to 4% non-denaturing PAGE analysis in TBE (45 mM Tris base, 45 mM boric acid, and 1 mM EDTA, pH 8.0), transferred to nylon membranes (Pierce), and DNA-bound proteins were visualized using the enhanced chemiluminescence (ECL) detection system (Millipore).

Chromatin Immunoprecipitation (ChIP)—ChIP analysis was performed using the EZ-ChIP^{TM} kit (Millipore). Briefly, HCT116 cells were fixed in 1% (v/v) formaldehyde for 10 min at room temperature. Cross-linked DNA was extracted and sheared by sonication using a Bioruptor (Cosmo Bio, Tokyo, Japan). Sheared DNA (amounts equivalent to that from 2×10^6 cells) was subjected to immunoprecipitation using 5 μg of indicated antibodies. After reversal from cross-linking and purification, fragmented DNA (2-μl aliquots) was subjected to 32 cycles of PCR amplification using the following primer pairs designed to amplify a region corresponding to −116 to +10 bp of the *HDM2*-P2 promoter: 5′-GACTCAGCTTTTCCTCTTGAGC-3′ (forward) and 5′-CTGAACACAGCTGGGAAAATG-3′ (reverse). The PCR reaction products were resolved via 2% agarose gel electrophoresis.

Luciferase Assays—HCT116 p53$^{+/+}$ and HCT116 p53$^{-/-}$ cells were cultured in 12-well culture plates and transfected using Gene-Juice Transfection Reagent (Novagen) following the manufacturer's instruction. In brief, 8×10^4 cells/well were cotransfected with 1 μg of hdm2p2luc01-WT or hdm2p2luc01-MU and indicated amounts of pcDNA-AP-4 plasmid. Empty vector pcDNA^{TM} 3.1/*myc*-His (−) A was added to each reaction such that a constant amount of DNA was

transfected. As an internal control, 50 ng of pRL-TK vector (Promega) expressing *Renilla* Luciferase under control of thymidine kinase promoter was included in each reaction. After 48 h of transfection, the cells were harvested, and luciferase activities were measured using the Dual-Luciferase Reporter Assay System (Promega). *Firefly* luciferase activity was normalized to that from *Renilla* luciferase, and the data represent mean-fold activity ($\pm$S. D.) relative to control transfections. All experiments were performed in triplicate.

DNA Pull-down Assay—Complementary double-stranded oligonucleotides corresponding to the -43 to -20 region of the *HDM2*-P2 promoter containing a WT (sense strand: 5′-biotin-GATCACTT-GTCTCC*CAGCTG*GGGCTATTT-3′) or MU (sense strand: 5′-biotin-GATCACTTGTCTCG*GAATTC*GGGCTATTT-3′) E-box sequence was prepared by Bio Basic Inc. MatInspector (39) was used to verify that disruption of the E-box in the MU DNA did not introduce new transcription factor binding sites. Double-stranded oligonucleotides were conjugated with MagnaBind^{TM} streptavidin beads (Pierce). The concentration of conjugated DNA was 6 fmol/μg of MagnaBind streptavidin beads. Nuclear extracts from 1×10^7 HCT116 p53$^{+/+}$ cells ($\sim$200 μg) were incubated at a 250:1 (w/w) ratio with poly(deoxyinosinic-deoxycytidylic) acid in binding buffer containing 20 mM HEPES-KOH (pH 7.9), 1.5 mM MgCl$_2$, 100 mM NaCl, 0.1% (v/v) Nonidet P-40, and protease inhibitor mixture (Calbiochem) at room temperature for 10 min, followed by addition of 10-μg MagnaBind streptavidin beads conjugated with either WT or MU oligonucleotides ($\sim$60 fmol DNA) at room temperature for 30 min. Bead-bound complexes were washed three times with the binding buffer and eluted using SDS sample buffer (65 mM Tris, pH 6.8, 2% SDS, 10% (v/v) glycerol, 0.05% bromphenol blue, and 0.3 M β-mercaptoethanol) at 95 °C for 5 min.

For cICAT and iTRAQ analyses, large-scale DNA pull-downs were performed as above except nuclear extracts from $\sim 4 \times 10^9$ HCT116 p53$^{+/+}$ cells ($\sim$140 mg of total protein) were harvested, and equal amounts ($\sim$70 mg each) were incubated with 25 nmol of bead-bound WT or MU oligonucleotide. Bound proteins were eluted using 100 mM Tris-HCl (pH 7.3), 5 mM EDTA, 0.05% SDS, and 8 M urea at room temperature for 30 min. Eluted protein concentrations were determined using the BCA assay reagent (Pierce).

cICAT Labeling and Fractionation by SCX Chromatography—For cICAT labeling, 200 μg of the eluted protein from large-scale DNA pull-downs prepared using WT or mutant DNA was labeled with light or heavy cICAT reagents, respectively (Applied Biosystems, Foster City, CA). The cICAT labeling reactions were performed as described (40). In brief, each protein sample was reduced with 1.25 mM TCEP-HCl and subsequently labeled with the cICAT reagents at 37 °C for 2 h. Labeled samples were combined and subjected to trypsin digestion (20:1 (w/w) protein:trypsin) at 37 °C for 16 h. The digested cICAT-labeled peptide mixtures were resuspended in buffer A (5 mM K$_2$HPO$_4$, pH 3.0, and 25% ACN) and fractionated by SCX chromatography using a 2.1 $\times$ 200 mm polysulfoethyl A SCX column (Poly LC, Columbia, MD). Gradient elution was performed at a flow rate of 1 ml/min using 0–25% buffer B (5 mM K$_2$HPO$_4$, pH 3.0, 25% ACN, and 350 mM KCl) over 30 min followed by 25–100% buffer B over 20 min. The cICAT-labeled peptides in the SCX fractions (retention time: 20–60 min) were further purified by avidin-affinity chromatography (Applied Biosystems). The purified cICAT-labeled peptides were dried by vacuum centrifugation, dissolved in cleaving reagents, and incubated in the dark at 37 °C for 2 h. After desalting using a ZipTip$_{C18}$ (Millipore), peptides were dried and subjected to duplicate LC-MS/MS analyses.

iTRAQ Labeling and Fractionation by SCX Chromatography—For iTRAQ labeling, 200 μg of eluted protein from large-scale DNA pull-downs prepared using WT or MU DNA beads were first subjected to gel-assisted digestion (41) to remove any buffer components that would interfere in the downstream iTRAQ labeling procedure. In brief, each sample was chemically reduced using 5 mM TCEP-HCl and alkylated using 10 mM methyl methanethiosulfonate at room temperature for 30 min. The alkylated protein sample was mixed with 17.5 μl of acrylamide/bisacrylamide solution (40%, v/v, 29:1), 2.5 μl of 10% (w/v) ammonium persulfate, and 1.07 μl of TEMED to form a gel matrix. The resulting gel was cut into small pieces and washed several times using 25 mM TEABC containing 50% (v/v) ACN. The gel samples were further dehydrated using 100% ACN and dried under vacuum. Trypsin digestion (20:1 (w/w) protein:trypsin) of gel samples was performed in 25 mM TEABC at 37 °C for 16 h. Peptides were extracted from the gel using 50% ACN containing 5% (v/v) FA, vacuum dried, and reconstituted in 30 μl of 25 mM TEABC.

To label peptides with the iTRAQ reagents (Applied Biosystems), one unit of labeling reagent (defined as the amount of reagent required to label 100 μg of protein) was reconstituted in 70 μl of ethanol. In this study, products isolated from duplicate WT DNA-bead reactions were labeled with iTRAQ^{114} and iTRAQ^{115}, whereas products isolated from duplicate MU DNA-bead reactions were labeled with iTRAQ^{116} and iTRAQ^{117}, respectively. After incubation at room temperature for 1 h, labeled peptides were pooled, resuspended in buffer A (1 ml final volume), and fractionated by SCX chromatography as described above.

LC-ESI-MS/MS Analysis—Vacuum-dried cICAT- and iTRAQ-labeled samples were reconstituted in 10 μl of buffer A (0.1% (v/v) FA in H$_2$O) and analyzed by nanoLC-MS/MS. Samples were injected into a 20 mm $\times$ 100 μm capillary trap column (Magic C$_{18}$; Michrom BioResources, Auburn, CA), separated using a 100 mm $\times$ 75 μm capillary column (Magic C$_{18}$; Michrom BioResources), and eluted using a linear gradient of 12–32% buffer B (0.1% (v/v) FA in ACN) over 50 min at 200 nl/min. An HP 1100 solvent delivery system (Hewlett-Packard, Palo Alto, CA) was used with post-column flow splitting interfaced to a QSTAR Pulsar *i* mass spectrometer (Applied Biosystems). Peptide fragmentation by collision-induced dissociation was performed automatically using information-dependent acquisition (Analyst QS v1.1, Applied Biosystems). The method applied one 1-s TOF MS scan and automatically switched to three 1.5-s product ion scans (MS/MS) when a target ion reached an intensity threshold of 20 counts. TOF MS scanning was performed over the range 400–1600 *m/z* using a Q1 transmission window of 380 amu (100%). Product ion scans were performed over the range 110–1600 *m/z* at low resolution utilizing Q2 transmission windows of 90 amu (25%), 165 amu (25%), 330 amu (25%), and 660 amu (25%).

Data Processing and Quantitative Analysis—For protein identification, data files from LC-ESI-MS/MS were batch searched against the Swiss-Prot sequence database v54.2 using the MASCOT v2.2.1 program (Matrix Science, London, UK). The peak list from MS/MS spectra generated by QSTAR Pulsar *i* was extracted using Analyst QS v1.1 with the charge state set to 2+, 3+, and 4+. MS and MS/MS centroid parameters were set to 50% height percentage and a merge distance of 0.1 amu. For MS/MS grouping, the averaging parameters were used by rejecting spectra with less than five peaks or precursor ions with less than 30 counts per second. The precursor mass tolerance for grouping was set to 0.01 Da, and both the maximum and minimum number of cycles per group was set to 1. Search parameters for peptide and MS/MS mass tolerance were $\pm$ 0.5 Da and $\pm$ 0.3 Da, respectively, with allowance for two missed cleavages from the trypsin digestion. Variable modifications for cICAT analysis were ICAT-C (Cys), ICAT-C:13C (9) (Cys), and oxidation (Met), whereas the variable modifications for iTRAQ analysis were deamidation (Asn, Gln), oxidation (Met), iTRAQ (N-terminal), iTRAQ (Lys), and methyl methanethiosulfonate (Cys). Peptides were considered identified if the MASCOT individual ion score was higher than the MASCOT identity score ($p <$ 0.05). The false discovery rate for peptide matches above the cut-off

threshold in this study was 2.18% for cICAT and 2.04% for iTRAQ. Under the indicated false discovery rate, proteins with scores ≥25 (for cICAT) and ≥40 (for iTRAQ) were confidently assigned.

For protein quantification, the ASAPRatio program (42) and the Multi-Q program (43) were used for cICAT and iTRAQ, respectively. First, the raw data files from QSTAR Pulsar *i* were converted to .mzXML format by the mzwiff v4.0.2 program (Seattle Proteome Center, Seattle, WA), and the MASCOT search results were exported in .xml data format. After the data conversions, ASAPRatio and Multi-Q were used to select unique cICAT- and iTRAQ-labeled peptides with confident MS/MS identification to detect signature ions (m/z = light and heavy for cICAT; 114, 115, 116, and 117 for iTRAQ), to apply a statistical method for the identification of outliers to be excluded from protein quantification, and to perform automated quantitation of peptide abundance (42, 43). All the differentially enriched proteins and corresponding peptides were manually verified. To calculate average protein ratios, the ratios of quantified unique cICAT and iTRAQ peptides were weighted according to their peak areas (for cICAT) or peak intensities (for iTRAQ).

Western Blotting—To measure histone H3 hyper-acetylation, HCT116 p53$^{+/+}$ cells were transfected as described in luciferase assays. At 24-h post-transfection, the cells were treated with the indicated amounts of TSA and further cultured for 8 h, 24 h, and 48 h, then harvested and washed three times with ice-cold phosphate-buffered saline. Total cell lysates were prepared by resuspending the cells in the SDS sample buffer, sonicating using a Bioruptor, and heating at 95 °C for 5 min. For verification of proteins associated with *HDM2*-P2 promoter sequences, DNA pull-down samples were prepared as described above. Protein samples were subjected to 10% SDS-PAGE analysis and transferred to polyvinylidene fluoride membranes (Millipore). The membranes were incubated with blocking buffer containing 5% (w/v) non-fat milk in TBS with 0.05% (v/v) Tween 20 (TTBS) at room temperature for 1 h, washed with TTBS three times at room temperature for 5 min, and then incubated with the antibodies in blocking buffer at 4 °C for 16 h with gentle agitation. Membranes were washed four times in TTBS at room temperature for 5 min and incubated with a 1:5000 dilution of secondary antibody (goat anti-mouse, donkey anti-goat, or goat anti-rabbit) conjugated with horseradish peroxidase (Santa Cruz Biotechnology) in blocking buffer. The resulting membranes were washed four times in TTBS at room temperature for 5 min, and immunopositive bands were visualized using the ECL detection system.

RESULTS

Identification of an HDM2-P2 Promoter E-box Responsible for p53-independent Transcriptional Repression by AP-4—It is well established that transcription of *HDM2* is mediated by a constitutive P1 promoter and an inducible P2 promoter (44). In response to DNA damage, p53 induces *HDM2* transcription by binding to the p53 responsive element (RE) located in the P2 promoter (44). In contrast, a UV-responsive *cis*-element immediately downstream of the p53 RE was reported to mediate repression of *HDM2* transcription in response to UV damage prior to p53-mediated activation (45, 46). Examination of the *HDM2*-P2 promoter revealed a putative E-box sequence (−29 to −34 bp relative to the transcription start site, CAGCTG) located within this UV-responsive *cis*-element (Fig. 1*A*) (21). In previous studies, AP-4 is highly expressed in colorectal carcinomas (12). In addition, transfection of HCT116 p53$^{-/-}$ cells, a p53-null derivative from the colorectal cancer cell line HCT116 (47), with an AP-4 expression plasmid

resulted in a decrease of HDM2 protein levels (25). Therefore, we chose the HCT116 cell line as our model system.

First, EMSA were performed to examine AP-4 binding to the predicted E-box sequence. Fig. 1*B* indicates that nuclear extracts from HCT116 p53$^{-/-}$ cells transiently over-expressing AP-4 shifted the WT E-box derived from the *HDM2*-P2 promoter (*lane 3*). Addition of unlabeled oligonucleotide containing WT (5′-CAGCTG-3′) E-box sequence into the reaction competed the observed EMSA shift (*lanes 4–7*) whereas no change was observed for oligonucleotide containing the MU (5′-GAATTC-3′) E-box, demonstrating that the AP-4-containing nuclear extract specifically associated with the identified E-box. To investigate whether the EMSA shift was AP-4-dependent, anti-AP-4 antibody was added to the EMSA reaction. As shown in *lane 9* of Fig. 1*B*, a supershifted band was observed, indicating that AP-4 was present in the complex bound to the E-box of the *HDM2*-P2 promoter *in vitro*.

To assess whether AP-4 bound to the identified E-box *in vivo*, ChIP assays were performed using rabbit or goat anti-AP-4. As shown in Fig. 1*C*, ectopically expressed AP-4 bound to the E-box region of endogenous *HDM2*-P2 promoter. In addition, co-transfection of AP-4 dose-dependently repressed the luciferase activity of the WT *HDM2*-P2 promoter reporter, whereas the mutated E-box sequence did not support repression (Fig. 1*D*). Importantly, no difference between HCT116 p53$^{+/+}$ and p53$^{-/-}$ cells was observed in the inhibition of *HDM2* transcription, indicating that the observed repression by AP-4 was p53-independent (Fig. 1*D*). Together these data indicated that AP-4 represses *HDM2* transcription by binding to the newly identified E-box of the *HDM2*-P2 promoter in a p53-independent manner.

Identification of HDM2-P2 Promoter-bound AP-4 Complex Components Using Complementary Quantitative Proteomics—Biochemical analyses have shown that AP-4 contains multiple protein-protein interaction domains that potentially promote either homo- or hetero-dimerization (1, 18). To identify proteins specifically associated with AP-4 and that participate in AP-4-mediated repression of *HDM2*, we adapted a single-step DNA-affinity purification strategy using nuclear extracts and *HDM2*-P2 promoter sequences containing the identified WT (5′-CAGCTG-3′) or MU (5′-GAATTC-3′) E-box sequences followed by quantitative comparison. It has been well documented that a combination of different isotope labeling methods targeting different amino acid residues, such as cICAT tagging on cysteine residues and iTRAQ tagging on N-terminal and lysine residues, provides a complementary and sequence-dependent analysis of interacting partners within a protein complex (48, 49). To identify as many AP-4 partners as possible, complementary cICAT and iTRAQ labeling strategies followed by two-dimensional LC-MS/MS analysis were performed to identify E-box-bound AP-4-interacting proteins.

After the single-step DNA affinity purification, proteins were eluted from magnetic beads, conjugated with WT or MU DNA,
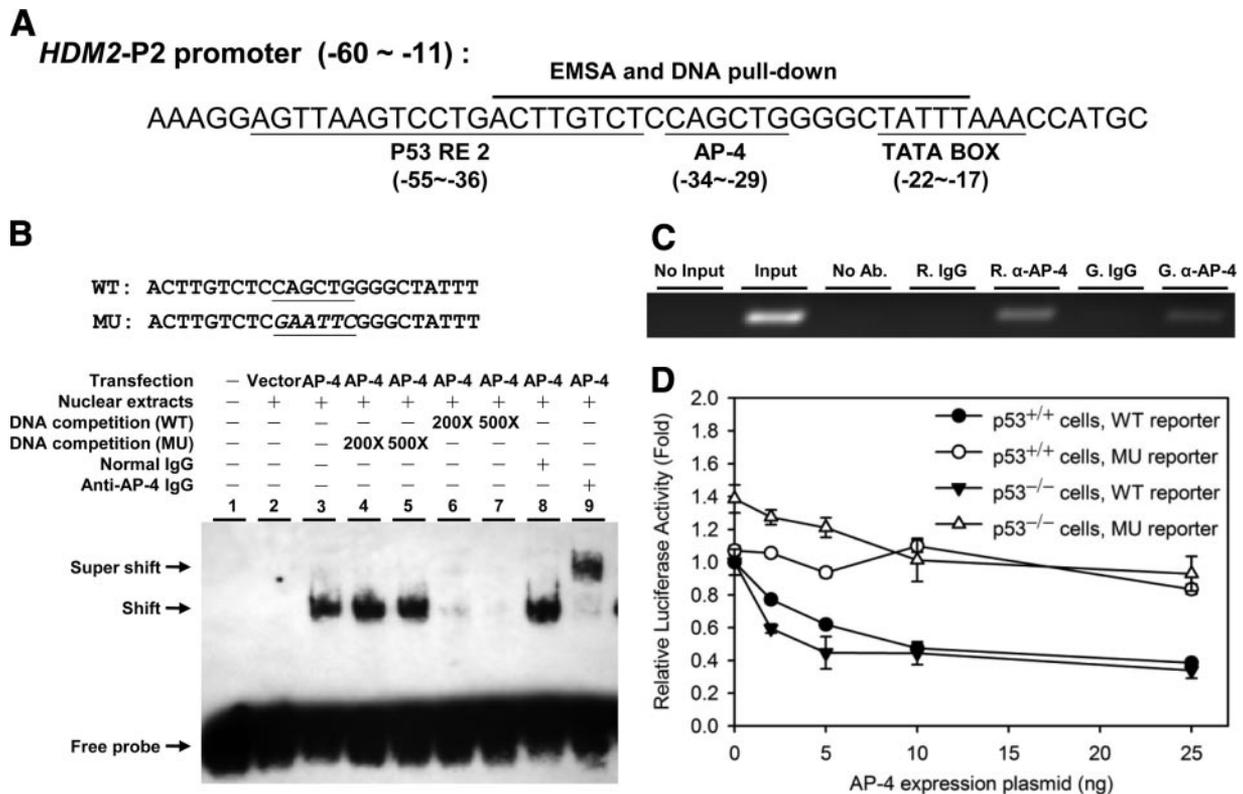
FIG. 1. **Identification of a functional AP-4 binding site in the *HDM2*-P2 promoter.** *A*, DNA sequence within the *HDM2*-P2 promoter containing a putative E-box (37). The oligonucleotide sequence used for EMSAs and DNA pull-downs is indicated. *B*, EMSA analysis of *HDM2*-P2 E-box oligonucleotide binding by AP-4; biotin-labeled *HDM2*-P2 E-box oligonucleotides were incubated with HCT116 p53^{−/−} nuclear extracts transiently transfected with pcDNA™ 3.1/*myc*-His (−) A empty vector (*lane 2*) or pcDNA-AP-4 plasmid (*lanes 3–9*). Excess unlabeled competitor DNA containing the WT (*lanes 6* and *7*) or MU (*lanes 4* and *5*) E-box was added to reactions to determine binding specificity. Identification of AP-4 in the complex was determined by addition of normal goat IgG (control, *lane 8*) or goat anti-AP-4 antibody (super shift, *lane 9*) to binding reactions. WT and MU sense strand oligonucleotide sequences are shown at the *top*. *C*, ChIP analysis demonstrating AP-4 binding at the *HDM2*-P2 promoter *in vivo*. Rabbit anti-AP-4 (R. α-AP-4) or goat anti-AP-4 (G. α-AP-4) antibody was used to precipitate DNA-cross-linked AP-4 from AP-4-overexpressing HCT116 cells prior to PCR amplification; normal rabbit (*R. IgG*) or goat (*G. IgG*). IgG was used as a negative control. *D*, luciferase assay demonstrating E-box-mediated repression of the *HDM2*-P2 promoter. Increasing amounts of pcDNA-AP-4 plasmid were transiently cotransfected with hdm2luc01-WT reporter (wild-type AP-4 E-box; *filled symbols*) or hdm2luc01-MU reporter (mutant E-box; *open symbols*) in HCT116 p53^{+/+} cells (*circles*) or HCT116 p53^{−/−} cells (*triangles*). After 48 h, total cell lysates were prepared and assayed for luciferase activity. Values represent mean-fold change ± S. D. (*n* = 3).

and subjected to cICAT and iTRAQ labeling. For cICAT labeling, proteins eluted from WT or MU DNA beads were labeled with light (L) or heavy (H) cICAT reagents, respectively. Because iTRAQ allows parallel four-plexed analysis, two replicate batches of proteins eluted from WT DNA beads were labeled with iTRAQ[114] and iTRAQ[115] reagents, and two replicate batches of proteins eluted from MU DNA beads were labeled with iTRAQ[116] and iTRAQ[117] reagents. The ratio of iTRAQ[116]/iTRAQ[117] can provide additional information of experimental errors during DNA pull-down, trypsin digestion, and iTRAQ labeling. The iTRAQ[116]/iTRAQ[117] ratio determined in this study ranges from 0.95 to 1.32 (supplemental Table 2). After duplicate LC-MS/MS analysis, 542 and 879 proteins were quantified using cICAT and iTRAQ labeling methods, respectively. The false discovery rate ($p < 0.05$) for peptide matches above the cut-off threshold was 2.18% for cICAT and 2.04% for iTRAQ. As expected, the majority of the

quantified proteins interacted with both DNA sequences in a nonspecific manner (enrichment ratio ≈1), highlighting the challenge of inherent background complexity in the characterization of DNA-protein complexes (26). Notably, the identified E-box lies adjacent to the TATA box and the p53 RE in the *HDM2*-P2 promoter (Fig. 1A). Therefore, among the nonspecific-binding proteins, those associated preferentially with the TATA box and p53 RE, such as TBP and p53, were identified. Because TATA box- and p53 RE-associated proteins were recruited independently of the E-box mutation, these proteins had enrichment ratios close to 1.0. Based on the three standard deviations model for the determination of fold-change thresholds ($p = 0.01$) (40, 41, 43), a protein enrichment ratio of ≥1.6-fold using WT DNA beads was considered statistically significant. Under this cut-off threshold, 75 proteins were considered putative AP-4-interacting proteins among the 1085 quantified proteins. Surprisingly, only

35 proteins were commonly identified by both labeling methods; 22 distinct proteins were identified using cICAT whereas 18 distinct proteins were identified using iTRAQ (Table I). The data presented herein strongly support the complementary nature of cICAT and iTRAQ labeling methods (48, 49).

Next, molecular functions and protein-protein interactions of the 75 differentially enriched proteins were further explored using Ingenuity Pathways Analysis (Ingenuity® Systems). To differentiate proteins preferentially bound to the E-box from those bound to the adjacent TATA box and p53 RE (Fig. 1*A*), TBP and p53 were included in the analysis. As shown in functional categorization summarized in Fig. 2, only a relatively small number of proteins were categorized as p53 and/or TBP direct-interacting proteins (8 proteins for TBP alone, 5 proteins for p53 alone, and 2 proteins for both TBP and p53). For example, the known TBP-interacting protein NFATC2 was significantly enriched in both cICAT and iTRAQ experiments (50). After filtering the previously documented p53- and TBP-interacting proteins, the majority of the 75 enriched proteins were categorized as putative AP-4-interacting proteins. Interestingly, 13 known DNA damage-responsive proteins, including APEX1, BRCA1, HMGB1/2/3, TERF2, TERF2IP, PCNA, POLE2, and RAD50, were the most significantly enriched proteins, implying a role for the AP-4 complex in regulating *HDM2*-P2 transcription during the DNA damage response (Fig. 2 and Table I). In addition to AP-4, 19 transcription factors, including the known AP-4-interacting protein SP1 (19), and 7 transcriptional repressors or corepressors, including CTCF and ZBTB7A, were also enriched; most of them have not previously been reported to interact, directly or indirectly, with AP-4. Furthermore, five histone-modifying proteins that function as transcriptional repressors were enriched. Among them, the histone methyltransferases EHMT1 and EHMT2 showed substantial enrichment, and histone deacetylases HDAC1 and HDAC2, which have been reported to associate with AP-4 in human immunodeficiency virus type 1 (HIV-1) (6), were moderately enriched in this study (Fig. 2 and Table I). Finally, two E-box binding bHLH transcription factors, USF2 and CLOCK, were also enriched (Fig. 2 and Table I).

To verify the advantage of complementary quantitative proteomics in the identification of AP-4 complex components, selected proteins exclusively enriched by the cICAT-labeling method, including CTCF, HMGB1, PCNA, and SP1, or those exclusively enriched by the iTRAQ-labeling method, including USF2, were further validated by Western blotting (Fig. 3). Several substantially enriched proteins common to both labeling methods were also examined, including AP-4, APEX1, and NFATC2. As expected, these proteins exhibited the highest WT DNA-bead enrichment ratios, confirming their specific recruitment by AP-4 to the *HDM2*-P2 promoter E-box (Fig. 3). Moderate enrichment of HADC1 and HDAC2 by AP-4 was also confirmed by Western blotting, consistent with the proteomic data. Finally, the binding of p53 to WT and MU DNA

beads was the same (enrichment ratio ≈ 1.0) (Fig. 3), further supporting p53-independent transcriptional repression of *HDM2* by AP-4.

Functional Domains of AP-4 Contribute to the Repression of HDM2 Transcription and AP-4 Complex Formation—In the above proteomic study, the enriched proteins may have been recruited either by virtue of direct DNA interactions or through protein-protein interactions with AP-4. Thus, we attempted to identify the functional domain(s) of AP-4 responsible for association with selected putative AP-4-interacting proteins and for repression of *HDM2* transcription. As shown in Fig. 4*A*, AP-4 contains several known domains, including a bHLH domain (residues 48–99), two distinct LR domains, LR1 (residues 99–120) and LR2 (residues 151–179), a Q/P-rich domain (residues 193–244), and an acidic domain (residues 289–339) (1). The bHLH domain is necessary for direct sequence-specific DNA binding (1), and both LR domains are required for the formation of the stable AP-4 homodimer (1) as well as for heterocomplex formation with GATA3 (19). The functions of the C-terminal Q/P-rich and acidic domains remain unknown; although they have been hypothesized to function as transcriptional activation domains (1).

We first identified domain(s) responsible for *HDM2* transcription repression using incremental AP-4 truncation mutants. As shown in Fig. 4, AP-4 truncation mutants conferred varying degrees of transcriptional suppression. The ChIP analysis shown in Fig. 4*B* revealed, as expected, that truncation of the N-terminal region containing the DNA binding bHLH domain (ΔN99, ΔN142, ΔN179) of AP-4 resulted in failure of *HDM2*-P2 promoter binding, whereas all AP-4 C-terminal truncation mutants (ΔC51, ΔC89, ΔC159, ΔC197, ΔC239) except ΔC239 were able to bind to the *HDM2*-P2 promoter. The failure of ΔC239 to bind to the *HDM2*-P2 promoter was because of the instability of the truncated protein (data not shown) and (Ref. 6). Luciferase reporter assays revealed that among the mutants capable of promoter binding, C-terminal truncation including deletion of the Q/P-rich domain resulted in the most substantial relief of gene repression (Fig. 4*C*).

We next investigated whether the Q/P-rich domain of AP-4 is responsible for association with the AP-4-interacting proteins enriched in the quantitative proteomic study, including APEX1, CTCF, HDAC1, and SP1. Plasmids encoding various AP-4 truncation mutants were transfected into HCT116 p53$^{+/+}$ cells, and DNA pull-down assays were performed using transfected cell nuclear extracts. As shown in Fig. 5, overexpression of full-length AP-4 led to increased recruitment of APEX1 to WT DNA beads compared with the AP-4 C-terminal truncation mutants ΔC89 or ΔC159. Notably, the same level of recruitment of APEX1 by the two AP-4 mutants and the endogenous AP-4 in the vector-only control was achieved, suggesting the considerable recruitment of APEX1 by endogenous AP-4 in the DNA pull-down assays. We also observed moderately increased recruitment of CTCF, HDAC1,

TABLE I

List of the potential AP-4-interacting proteins differentially bound to the HDM2-P2 promoter E-box sequence

Proteins from HCT116 p53^{+/+} cell nuclear extracts enriched on the *HDM2*-P2 promoter E-box sequence (enrichment ratio ≥ 1.6) were identified by quantitative proteomics using cICAT and iTRAQ labeling methods and were categorized according to their known molecular function(s). Complete information of enriched proteins labeled by cICAT and iTRAQ was summarized in supplemental Tables 1 and 2, respectively.

Protein name	Accession number	Gene name	Mass	cICAT			iTRAQ			
				Score[a]	Peptide[b]	WT/MU[c]	Score[a]	Peptide[b]	WT1/MU2[d]	WT2/MU2[d]
bHLH transcription factor										
Activating enhancer-binding protein 4	Q01664	TFAP4	38702	59	2	1.96 ± 0.07	199	3	2.46 ± 0.60	1.96 ± 0.39
Circadian locomoter output cycles protein kaput	O15516	CLOCK	95244	64	1	2.04 ± N/A	N/A	N/A	N/A	N/A
Upstream stimulatory factor 2	Q15853	USF2	36932	N/A[e]	N/A	N/A	108	4	3.36 ± 0.90	3.22 ± 0.71
Transcription factor										
Nuclear factor of activated T-cells, cytoplasmic 2	Q13469	NFATC2	100083	65	2	6.46 ± 2.10	88	3	2.00 ± 0.58	2.05 ± 0.49
Alpha-globin transcription factor CP2	Q12800	TFCP2	57220	1019	32	3.32 ± 1.58	522	9	2.26 ± 0.34	2.00 ± 0.33
General transcription factor II-I	P78347	GTF2I	112346	141	3	3.15 ± 0.82	757	28	1.74 ± 0.33	1.63 ± 0.36
Upstream-binding protein 1	Q9NZI7	UBP1	60453	903	40	2.70 ± 0.45	582	12	1.88 ± 0.19	1.73 ± 0.19
COUP transcription factor 1	P10589	NR2F1	46126	316	5	2.22 ± 2.13	143	3	2.13 ± 0.56	1.94 ± 0.49
COUP transcription factor 2	P24468	NR2F2	45542	228	2	1.78 ± 0.05	136	1	1.99 ± N/A	1.78 ± N/A
Nuclear factor 1 C-type	P08651	NFIC	55640	85	3	1.69 ± 0.18	175	2	1.73 ± 0.06	1.75 ± 0.05
Nuclear receptor subfamily 2 group F member 6	P10588	NR2F6	42952	78	3	4.28 ± 0.27	N/A	N/A	N/A	N/A
Homeobox protein PKNOX1	P55347	PKNOX1	47577	37	1	3.69 ± N/A	N/A	N/A	N/A	N/A
Stimulatory protein 1	P08047	SP1	80644	92	1	2.59 ± N/A	N/A	N/A	N/A	N/A
Nuclear factor 1 A-type	Q12857	NFIA	55909	75	2	2.10 ± 0.21	N/A	N/A	N/A	N/A
Breast cancer type 1 susceptibility protein	P38398	BRCA1	207592	38	1	2.03 ± N/A	N/A	N/A	N/A	N/A
Zinc fingers and homeoboxes protein 3	Q9H4I2	ZHX3	104592	60	2	1.82 ± 1.12	N/A	N/A	N/A	N/A
Zinc finger and BTB domain-containing protein 7B	O15156	ZBTB7B	57990	N/A	N/A	N/A	67	2	4.25 ± 0.74	4.19 ± 0.95
Transcription factor Sp3	Q02447	SP3	81876	N/A	N/A	N/A	110	2	2.60 ± 0.07	1.98 ± 0.03
Steroid hormone receptor ERR1	P11474	ESRRA	55404	N/A	N/A	N/A	50	1	1.76 ± N/A	1.99 ± N/A
DNA damage response protein										
DNA-(apurinic or apyrimidinic site) lyase	P27695	APEX1	35532	766	25	8.10 ± 3.21	782	26	4.58 ± 1.43	4.18 ± 1.62
Telomeric repeat-binding factor 2-interacting protein 1	Q9NYB0	TERF2IP	44233	66	3	5.73 ± 2.57	93	2	3.18 ± 0.76	4.39 ± 2.67
High mobility group protein B3	O15347	HMGB3	22965	85	2	5.51 ± 0.32	132	4	2.45 ± 0.30	2.33 ± 0.24
DNA topoisomerase 2-binding protein 1	Q92547	TOPBP1	170571	40	1	2.77 ± N/A	41	1	2.43 ± N/A	2.45 ± N/A
Mediator of DNA damage checkpoint protein 1	Q14676	MDC1	226529	278	16	1.92 ± 1.35	427	10	1.28 ± 0.21	1.34 ± 0.44
High mobility group protein B2	P26583	HMGB2	24019	497	1	10.01 ± N/A	N/A	N/A	N/A	N/A
DNA polymerase epsilon subunit 2	P56282	POLE2	59499	34	1	8.66 ± N/A	N/A	N/A	N/A	N/A
High mobility group protein B1	P09429	HMGB1	24878	603	9	5.37 ± 0.48	N/A	N/A	N/A	N/A
Proliferating cell nuclear antigen	P12004	PCNA	28750	202	8	3.12 ± 1.43	N/A	N/A	N/A	N/A
Poly(ADP-ribose) polymerase 2	Q9UGN5	PARP2	66164	45	2	1.73 ± 0.11	N/A	N/A	N/A	N/A
Telomeric repeat-binding factor 2	Q15554	TERF2	55517	N/A	N/A	N/A	188	7	3.96 ± 0.63	3.64 ± 0.40
High mobility group protein 1-like 10	Q9UGV6	HMG1L10	24203	N/A	N/A	N/A	48	1	2.08 ± N/A	2.31 ± N/A
DNA repair protein RAD50	Q92878	RAD50	153797	N/A	N/A	N/A	83	4	1.96 ± 0.27	1.81 ± 0.25
Repressor and corepressor										
Zinc finger and BTB domain-containing protein 7A	O95365	ZBTB7A	61401	886	15	5.66 ± 1.90	56	2	3.32 ± 0.26	3.09 ± 0.17
C-terminal-binding protein 1	Q13363	CTBP1	47505	40	1	2.27 ± N/A	177	5	1.68 ± 0.38	1.71 ± 0.12
Protein wiz	O95785	WIZ	178563	117	10	1.96 ± 0.40	801	26	1.68 ± 0.30	1.61 ± 0.25
CCCTC binding factor	P49711	CTCF	82732	34	1	9.68 ± N/A	N/A	N/A	N/A	N/A
Transcription factor CP2-like protein 1	Q9NZI6	TFCP2L1	54593	331	2	2.61 ± 0.38	N/A	N/A	N/A	N/A

TABLE I—*continued*

Protein name	Accession number	Gene name	Mass	cICAT			iTRAQ			
				Score[a]	Peptide[b]	WT/MU[c]	Score[a]	Peptide[b]	WT1/MU2[d]	WT2/MU2[d]
Paired amphipathic helix protein Sin3b	O75182	SIN3B	132983	N/A	N/A	N/A	87	3	1.77 ± 0.49	1.74 ± 0.71
Methyl-CpG-binding domain protein 2	Q9UBB5	MBD2	43228	N/A	N/A	N/A	147	3	1.64 ± 0.19	1.68 ± 0.25
SWI·SNF-related protein										
SWI·SNF-related matrix-associated actin-dependent regulator of chromatin subfamily B member 1	Q12824	SMARCB1	44113	69	4	2.97 ± 0.73	317	13	1.84 ± 0.29	1.77 ± 0.26
AT-rich interactive domain-containing protein 1A	O14497	ARID1A	241892	34	3	2.25 ± 0.25	367	10	1.79 ± 0.28	1.76 ± 0.24
SWI·SNF-related matrix-associated actin-dependent regulator of chromatin subfamily C member 2	Q8TAQ2	SMARCC2	132797	1529	51	2.07 ± 0.39	1430	30	1.64 ± 0.40	1.61 ± 0.36
SWI·SNF-related matrix-associated actin-dependent regulator of chromatin subfamily E member 1	Q969G3	SMARCE1	46621	71	4	2.03 ± 0.12	1142	28	1.88 ± 0.30	1.76 ± 0.28
AT-rich interactive domain-containing protein 2	Q68CP9	ARID2	197268	1226	42	1.95 ± 0.51	1357	50	1.80 ± 0.34	1.67 ± 0.30
Histone-modifiying protein										
Euchromatic histone-lysine *N*-methyltransferase 1	Q9H9B1	EHMT1	138166	1231	58	2.60 ± 1.02	226	7	2.05 ± 0.43	1.91 ± 0.42
Euchromatic histone-lysine *N*-methyltransferase 2	Q96KQ7	EHMT2	132287	870	37	2.45 ± 0.56	922	23	2.02 ± 0.32	1.83 ± 0.31
Histone deacetylase complex subunit SAP130	Q9H0E3	SAP130	110255	52	3	1.93 ± 0.25	79	2	1.37 ± 0.05	1.22 ± 0.12
Histone deacetylase 1	Q13547	HDAC1	55068	175	5	1.66 ± 0.22	808	15	1.71 ± 0.55	1.47 ± 0.28
Histone deacetylase 2	Q92769	HDAC2	55329	164	8	1.66 ± 0.19	631	8	1.29 ± 0.21	1.28 ± 0.20
Basic transcription machinery										
Transcription termination factor 2	Q9UNY4	TTF2	129508	43	2	1.73 ± 0.02	261	14	1.30 ± 0.22	1.21 ± 0.18
TATA-binding protein-associated factor 172	O14981	BTAF1	206756	97	4	1.70 ± 0.10	N/A	N/A	N/A	N/A
Others										
Deoxynucleotidyltransferase terminal-interacting protein 1	Q9H147	DNTTIP1	36990	481	12	4.80 ± 1.30	132	5	2.01 ± 0.63	1.83 ± 0.99
Serine/threonine-protein kinase VRK1	Q99986	VRK1	45447	124	3	4.14 ± 0.61	278	11	2.42 ± 0.42	2.28 ± 0.40
Zinc finger protein 462	Q96JM2	ZNF462	161426	95	3	3.62 ± 0.61	76	2	2.02 ± 0.20	1.90 ± 0.17
Bromodomain-containing protein 7	Q9NPI1	BRD7	74092	223	8	3.33 ± 0.95	207	8	1.77 ± 0.38	1.69 ± 0.24
UPF0609 protein C4orf27	Q9NWY4	C4orf27	39383	111	5	3.10 ± 1.37	240	8	1.80 ± 0.45	1.72 ± 0.46
Chromatin accessibility complex protein 1	Q9NRG0	CHRAC1	14701	330	9	2.67 ± 1.22	47	1	2.92 ± N/A	2.50 ± N/A
YEATS domain-containing protein 2	Q9ULM3	YEATS2	150688	97	4	2.26 ± 0.43	198	7	1.82 ± 0.38	1.62 ± 0.31
ZZ-type zinc finger-containing protein 3	Q8IYH5	ZZZ3	101960	94	3	1.96 ± 0.20	82	3	1.77 ± 0.10	1.60 ± 0.18
Protein S100-A8	P05109	S100A8	10828	56	1	8.91 ± N/A	N/A	N/A	N/A	N/A
Uncharacterized protein C14orf43	Q6PJG2	C14orf43	114918	158	6	2.67 ± 0.14	N/A	N/A	N/A	N/A
Zinc finger protein 335	Q9H4Z2	ZNF335	144802	57	2	2.55 ± 0.92	N/A	N/A	N/A	N/A
E3 ubiquitin-protein ligase UHRF2	Q96PU4	UHRF2	89928	182	5	1.92 ± 0.22	N/A	N/A	N/A	N/A
PR domain zinc finger protein 16	Q9HAZ2	PRDM16	140172	44	2	1.85 ± 0.02	N/A	N/A	N/A	N/A
Coiled-coil domain-containing protein 95	Q8NBZ0	INO80E	26462	295	14	1.76 ± 0.52	N/A	N/A	N/A	N/A
SAPS domain family member 3	Q5H9R7	SAPS3	97608	40	1	1.63 ± N/A	N/A	N/A	N/A	N/A
GTP-binding nuclear protein Ran	P62826	RAN	24408	N/A	N/A	N/A	45	1	2.86 ± N/A	1.68 ± N/A
Thymocyte nuclear protein 1	Q9P016	THYN1	25681	N/A	N/A	N/A	138	1	2.52 ± N/A	2.19 ± N/A
Calcineurin-binding protein cabin-1	Q9Y6J0	CABIN1	246197	N/A	N/A	N/A	51	1	2.07 ± N/A	1.75 ± N/A

TABLE I—*continued*

Protein name	Accession number	Gene name	Mass	cICAT			iTRAQ			
				Score[a]	Peptide[b]	WT/MU[c]	Score[a]	Peptide[b]	WT1/MU2[d]	WT2/MU2[d]
Cytoskeleton-associated protein 5	Q14008	CKAP5	225366	46	0	N/A	173	3	2.07 ± 0.14	2.12 ± 0.38
Neuron navigator 3	Q8IVL0	NAV3	255461	N/A	N/A	N/A	40	1	1.93 ± N/A	2.01 ± N/A
Ephexin-1	Q8N5V2	NGEF	82445	N/A	N/A	N/A	40	1	1.93 ± N/A	1.63 ± N/A
Spliceosome RNA helicase BAT1	Q13838	BAT1	48960	157	0	N/A	214	1	1.88 ± N/A	1.83 ± N/A
Metastasis-associated protein MTA3	Q9BTC8	MTA3	67461	N/A	N/A	N/A	95	2	1.82 ± 0.26	1.74 ± 0.07
Uncharacterized protein C6orf174 precursor	Q5TF21	C6orf174	103136	N/A	N/A	N/A	152	7	1.78 ± 0.17	1.67 ± 0.17

[a] Mascot protein score.
[b] The number of nondegenerate (unique) peptide used for quantification.
[c] cICAT ratios, WT and MU indicate proteins enriched on WT and MU DNA beads, respectively.
[d] iTRAQ ratios, WT1 and WT2, indicate proteins enriched on WT DNA beads, whereas MU1 and MU2 indicate proteins enriched on MU DNA-beads, respectively.
[e] Not available.
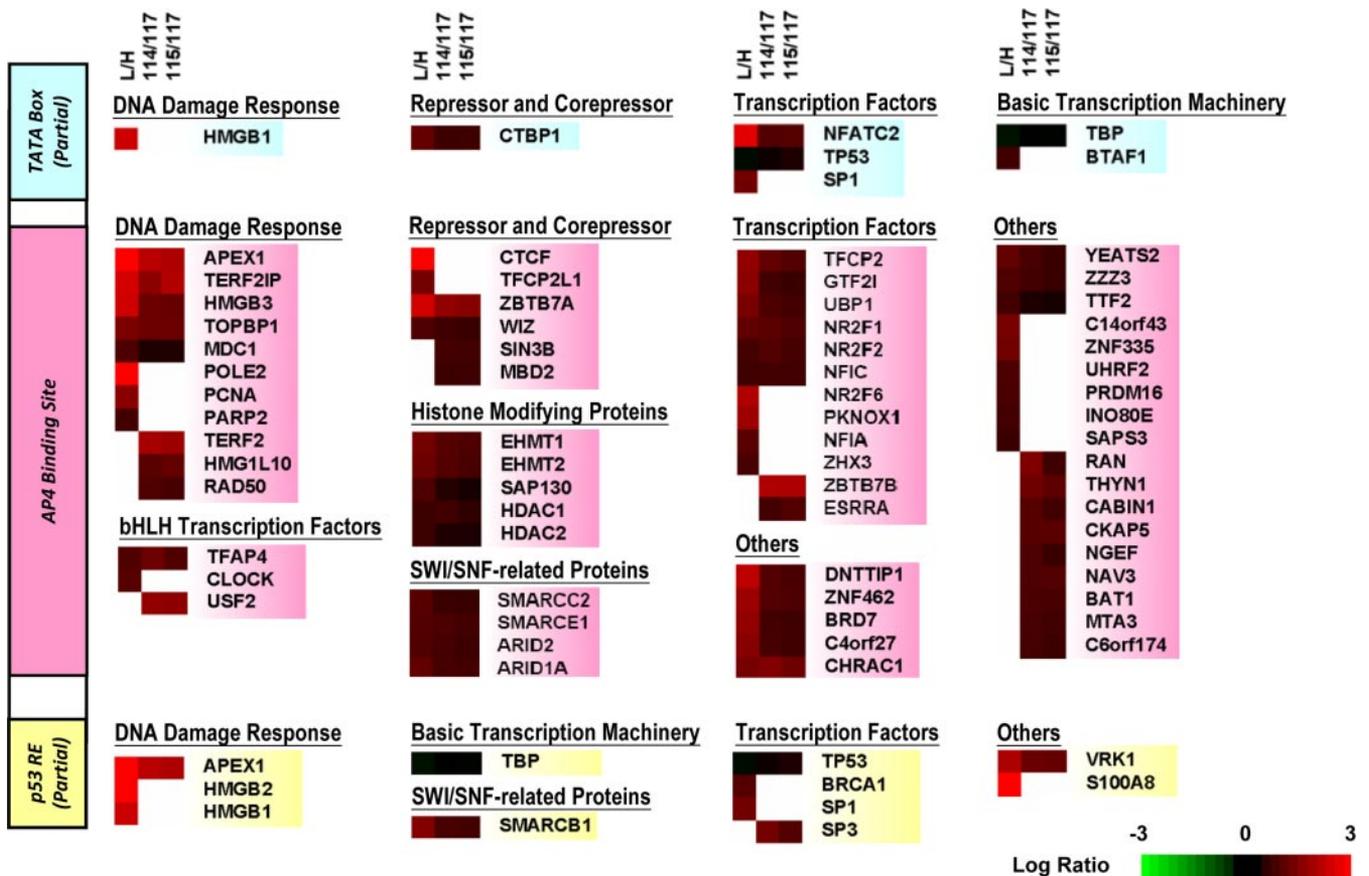
FIG. 2. **Heatmap representation of nuclear proteins differentially enriched on the *HDM2*-P2 promoter E-box.** Positively enriched proteins (enrichment ratio ≥ 1.6) identified from cICAT and iTRAQ labeling methods are classified in columns according to their known molecular functions. Proteins known to interact directly with p53 (*yellow*, bottom) and TBP (*blue*, top) were assigned to their corresponding partial binding site sequences; others were categorized as potential AP-4-interacting proteins (*red*, middle). For the cICAT experiment, proteins enriched on WT or MU DNA beads were labeled with light (*L*) or heavy (*H*) cICAT reagents, respectively. For iTRAQ experiments, proteins enriched on WT DNA beads were labeled with iTRAQ[114] and iTRAQ[115] reagents, whereas proteins enriched on MU DNA beads were labeled with iTRAQ[116] and iTRAQ[117] reagents, respectively.

and SP1 by the full-length AP-4 onto the WT DNA beads. These data confirmed the specific interaction between AP-4 and the selected proteins identified in the quantitative pro-

teomics study. Taken together with the observation that deletion of the AP-4 acidic region (mutants ΔC89 or ΔC159) resulted in loss of recruitment of the selected proteins of

FIG. 3. **Validation of AP-4 binding partners from cICAT and iTRAQ analyses by Western blotting.** Proteins enriched from HCT116 p53^{+/+} nuclear extracts by DNA pull-down (compare WT and MU) were analyzed by Western blotting using antibodies against selected proteins indicated at the *left*. The relative ratios of protein binding to WT and MU DNA-bead quantified by cICAT and iTRAQ analyses are shown at *right*. *N/A*, not available.

interest, these data demonstrate that the acidic region of AP-4 is critical for interaction with APEX1, CTCF, HDAC1, and SP1.

HDAC-independent Repression of HDM2 Transcription by AP-4—Among the previously reported mechanisms of mammalian transcriptional regulation, histone acetylation by HAT and deacetylation by HDAC are of critical importance because they modulate the accessibility of transcription factors to their DNA binding sites (51); a common feature of mammalian transcriptional repression is promoter-specific recruitment of HDAC. In our study, HDAC1 and HDAC2 were moderately enriched on WT DNA beads (Table I and Fig. 3), and HDAC1 was confirmed to interact with the C-terminal acidic region of AP-4 by Western blot analysis (Fig. 5). To examine whether HDAC is involved in AP-4-mediated repression of *HDM2* transcription, we cotransfected HCT116 p53^{+/+} cells with the *HDM2*-P2 luciferase reporter plasmid and the AP-4 expression plasmid in the presence of TSA, a specific inhibitor of HDAC. As shown in Fig. 6, incubation with TSA for 8 or 24 h resulted in dose-dependent hyper-acetylation of histone H3. To our surprise, however, TSA did not relieve AP-4-dependent repression of *HDM2* transcription (Fig. 6A). Because TSA is cytotoxic after prolonged treatment (52), measurement of luciferase activity from cells treated with TSA for more than 24 h was not possible. Although DNA pull-downs revealed specific recruitment of HDAC1 by AP-4 (Figs. 3 and 5), transient transfection assays suggested that AP-4 modulates *HDM2* expression through an HDAC-independent mechanism.

DISCUSSION

MS-based Comprehensive Identification of DNA-bound Protein Complex Using Complementary Isotopic Labeling Methods—In this study, we reported the first identification of AP-4 protein complex containing 75 putative components recruited to the *HDM2*-P2 promoter E-box sequence. Our data also demonstrated the first example to apply single-step
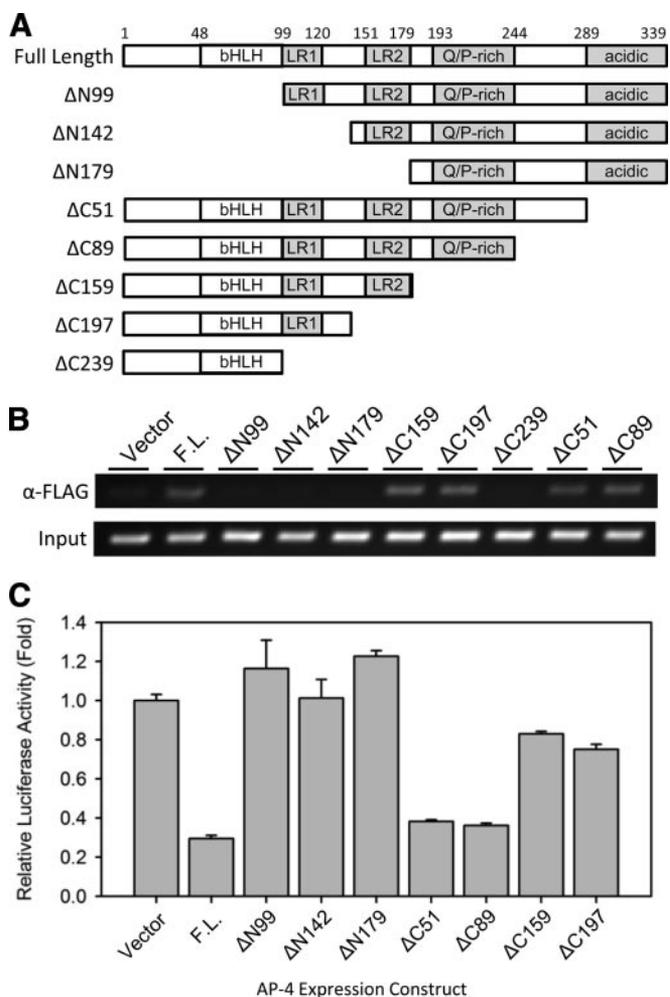
FIG. 4. **Analysis of *HDM2*-P2 promoter binding and transcriptional repression using AP-4 truncation mutants.** *A*, schematic representation of full-length AP-4 and AP-4 truncation mutant expression constructs. The AP-4 residue positions are indicated at the *top*. *bHLH*, basic helix-loop-helix domain; *LR1*, leucine repeat domain 1; *LR2*, leucine repeat domain 2; *Q/P-rich*, glutamine- and proline-rich domain. *B*, ChIP analysis demonstrating binding of FLAG-tagged full-length AP-4 and AP-4 truncation mutants at the *HDM2*-P2 promoter *in vivo*. Anti-FLAG antibody was used to precipitate DNA-cross-linked FLAG-AP-4 from HCT116 p53^{+/+} cells transfected with the indicated FLAG-AP-4 expression construct prior to PCR amplification. *C*, luciferase assay examining E-box-mediated repression of the *HDM2*-P2 promoter by AP-4 or AP-4 truncation mutants. HCT116 p53^{+/+} cells were cotransfected with hdm2luc01-WT reporter plasmid and the full-length (*F.L.*) pcDNA-AP-4 expression construct or the indicated AP-4-truncation mutant expression construct. After 48 h, the cells were harvested and subjected to luciferase assays. Values represent mean-fold activity relative to control (Vector)-transfected cells ± S. D. (*n* = 3).

DNA affinity purification from crude nuclear extracts followed by complementary quantitative proteomics, including cICAT and iTRAQ labeling methods, to achieve comprehensive identification of protein complex components. Quantitative proteomics using stable isotope labeling methods in combination with affinity purification has been widely used to characterize
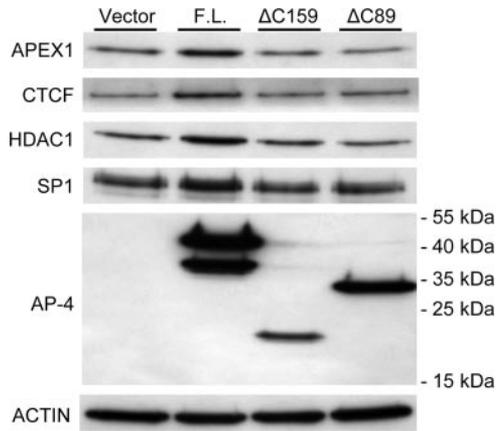
FIG. 5. **Comparison of AP-4 and AP-4 truncation mutant binding partners by Western blotting.** HCT116 p53$^{+/+}$ cells were transfected with empty vector, full-length (*F.L.*) AP-4 expression vector, or the indicated AP-4 truncation mutant expression constructs (*top*). After 48 h, nuclear extracts were prepared and subjected to DNA pull-down assays using WT DNA beads followed by Western blotting analysis using antibodies against selected proteins indicated at *left*. As a control, nuclear extracts were subjected to Western blotting using anti-actin antibody.
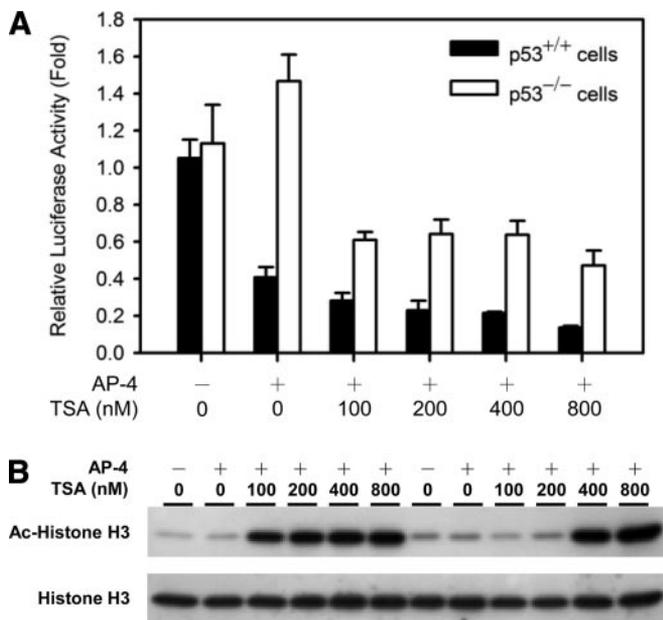
FIG. 6. **Effect of TSA on AP-4-mediated repression of *HDM2*-P2 transcription.** HCT116 p53$^{+/+}$ and p53$^{-/-}$ cells were cotransfected with the wild-type *HDM2*-P2 reporter (hdm2luc01-WT) and the pcDNA-AP-4 expression construct. After 24 h, the indicated amounts of TSA were added to transfection reactions and incubated for additional 8 h or 24 h. Cells were harvested and subjected to (*A*) luciferase assays or (*B*) Western blotting using antibodies against acetyl-histone H3 or histone H3.

DNA-bound protein complexes (26). For example, ICAT labeling in combination with single-step immunoprecipitation (31) or DNA affinity purification (32–36) has been used to identify DNA-bound protein complexes and to study the dynamics of the transcriptional machinery.

In principle, ICAT method detects only cysteine-labeled peptides enriched via biotin-avidin affinity purification, allowing significant reduction of sample complexity to enhance the probability of identifying low-abundance proteins such as transcription factor complexes (29, 33). However, cysteine abundance is relatively low in proteins, yielding low recovery of labeled proteins during biotin-avidin affinity purification (53, 54). The introduction of the iTRAQ method (30), which labels N-terminal and lysine residues, allows more sensitive and global analysis of protein complex components. These complementary labeling methods have been successfully applied to identify cancer markers in endometrial tissues, in which cICAT labeling enhances identification of signaling factors and low-abundance proteins, whereas iTRAQ labeling enhances transcription factor identification (49). In a recent proteomic study of butyrate-treated colorectal cancer cells, Tan *et al.* (55) also reported that cICAT and iTRAQ complementarily identified different proteins. In the present study, about half (35 out of 75) of the enriched proteins were detected and quantified by both labeling methods, whereas 22 and 18 of the 75 proteins were quantified only by cICAT and iTRAQ labeling, respectively. Because the complexity of the samples enriched via protein-DNA complex formation from nuclear extracts was greatly reduced compared with whole-cell proteomic analysis, our proteomics results did not reveal any distinct functional category for these uniquely identified proteins by each labeling method. Nevertheless, our study demonstrates the efficacy of complementary isotope labeling for identification of DNA-bound protein complex components.

Sequence-specific DNA-protein Complex Isolation Revealed by Biochemical versus MS-based Approaches—Purification of sequence-specific DNA binding transcription factors and their stably or dynamically associating protein partners faces the challenge of obtaining specific protein complex with minimal nonspecific interference. In classical biochemical approach, unbiased identification of sequence-specific DNA binding proteins requires several chromatographic separation steps followed by a final DNA affinity chromatography using cognate recognition sequence as a ligand. In addition to cell organelle differential centrifugation, several chromatographic steps, such as gel-filtration, heparin-affinity, or phosphocellulose P11, have been widely used as a prefractionation step prior to DNA affinity purification, allowing isolation of highly purified transcription factors (56, 57). In a recent study of Yaneva and Tempst (58), a prefractionation of crude nuclear extracts using phosphocellulose P11 chromatography followed by DNA affinity purification has been successfully applied for MALDI-TOF and TOF/TOF MS-based identification of transcription factors. However, the multi-step biochemical purification procedure is typically laborious and suffers from low purification yield as well as potential disruption of protein-protein interaction by stringent washing/elution conditions, *e.g.* high salt washes, hampering the dynamics

Fig. 7. **Schematic diagram depicting possible mechanisms of AP-4-mediated *HDM2* transcription repression revealed by complementary quantitative proteomics.** Proteins from HCT116 p53$^{+/+}$ cell nuclear extracts with enriched binding to the WT *HDM2*-P2 promoter sequence were evaluated via complementary quantitative proteomics. Resulting proteins of interest are depicted in the diagram at different distances from AP-4 according to their enrichment ratio (varying shades of *red*). Molecular functions are indicated by the outline *colors*.
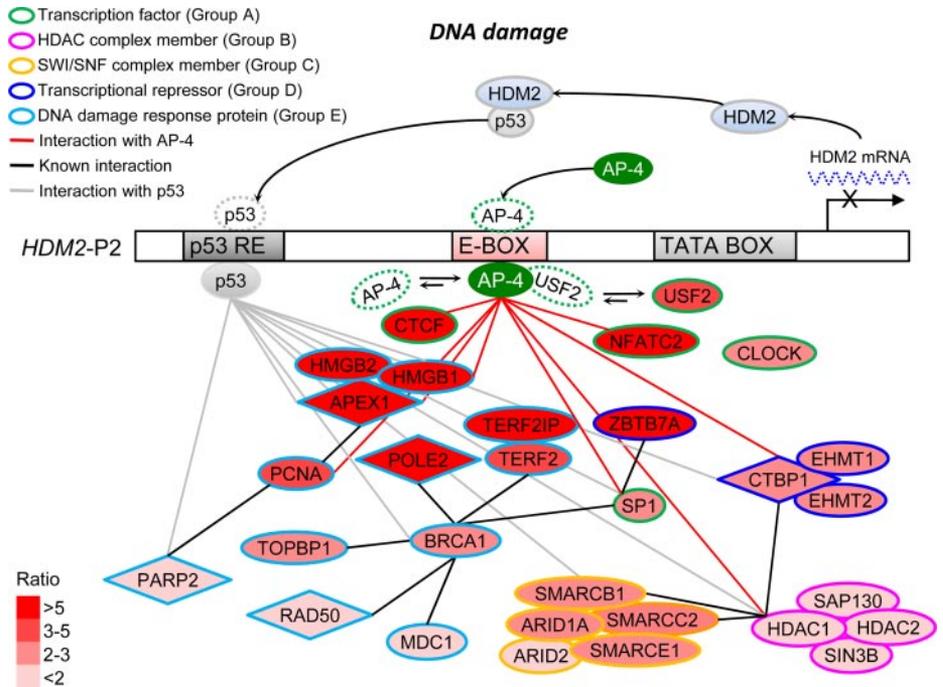
studies of transcription factor complex in response to environmental stimuli.

In contrast, quantitative proteomics using stable isotope labeling in combination with single-step DNA affinity purification from crude nuclear extracts has been developed to characterize novel transcription factor binding to a DNA sequence of interests (35, 36) and to study the dynamics of transcription factor complex (32–34, 59, 60). By taking the advantages of quantitative comparison on the recruited proteins from wild-type *versus* mutant DNA sequences, specific DNA-binding proteins can be effectively discriminated from nonspecific co-purifications. Compared with commonly used biochemical multi-step purification methods, in general, the "brute-force" single-step DNA affinity purification followed by quantitative proteomics offers advantages of relatively simple purification process and less amount of starting materials. By applying appropriate washing conditions, such as stringent negative/positive selection using WT and MU DNA sequences (35, 36) or mild washes using binding buffer (32–34, 59, 60), candidate transcription factor or its associated protein complex binding to functional DNA elements can be identified. Despite these successes, there are several drawbacks regarding the MS-based approach. Biochemical validations are still required to exclude false-positive and false-negative identifications (60), In addition, these approaches are usually applicable in few expert laboratories with sophisticated instrumentation and bioinformatic support.

Taken together, therefore, optimal purity for characterization of transcription factor and its association complex may be achieved by combined use of classical biochemical purifications, DNA affinity purification, and mass spectrometric identification. When the protein abundance is a critical issue, quantitative proteomics approaches utilizing isotopic labeling methods offer an alternative with better sensitivity to identify unknown binding partners or to study the dynamic changes of proteins complex from a known transcription factor.

Functional Implications of AP-4 Protein Complex on HDM2 Repression—Based on our data and previous studies, we propose potential mechanisms of *HDM2* transcription repression by AP-4 are presented in Fig. 7. The differentially recruited proteins in the AP-4 complex were categorized into five groups according to known molecular functions and protein-protein interactions: transcription factors (group A), HDAC complex members (group B), SWI·SNF complex members (group C), transcriptional repressors (group D), and DNA damage response proteins (group E). The transcriptional repressors can be further categorized as active repressors, which bind specific DNA sequences to recruit corepressors for inhibition of target gene expression, or as passive repressors, which likely sequester bHLH activator proteins through nonfunctional heterodimer formation. The potential mechanisms of AP-4-mediated *HDM2* repression are elaborated as follows:

I. Passive Repression by Competition or Coordination with Other Transcription Factors—It is well recognized that mammalian transcription repression can be mediated by passive repressor proteins (51). Passive repressor proteins inhibit transcription by binding to and forming inactive heterodimers with transcriptional activators or by sequestering co-activators required for transcription activation (51). For example, transcription factor MafG forms homodimer and competes with MafG/p45 heterodimer for binding to Maf recognition

TABLE II

Putative transcription factor binding sites in HDM2-P2 promoter analyzed by the MatInspector program

The DNA sequence of the HDM2-P2 promoter (Chr. 12, contig NC_000012, 67488540−67489062, 523 bp) was analyzed by MatInspector using MatInspector library version 7.1 with an optimized matrix threshold of 0.80.

Family/Matrix[a]	Optimized matrix similarity threshold[b]	Position[c]	Strand[d]	Matrix similarity[e]	Sequence
AP-4					
V$AP4R/V$AP4.01	0.85	−40 ~ −24	(−)	0.939	agcccCAGCTGgagaca
CTCF					
V$CTCF/V$CTCF.01	0.80	−305 ~ −281	(+)	0.820	ctctcgcggcggtgGGGGtgggggt
V$CTCF/V$CTCF.01	0.80	−247 ~ −223	(+)	0.815	ggtcacgggggccgGGGGctgcggg
NFATC2					
V$NFAT/V$NFAT.01	0.95	−118 ~ −100	(−)	0.965	agaGGAAaagctgagtcaa
SP1					
V$SP1F/V$SP1.01	0.88	−327 ~ −313	(+)	0.911	aggaGGGCgggattt
V$SP1F/V$SP1.01	0.88	−243 ~ −229	(+)	0.896	acggGGGCcgggggc
V$SP1F/V$SP1.01	0.88	−152 ~ −138	(+)	0.911	gtctGGGCgggattg
V$SP1F/V$SP1.02	0.85	−407 ~ −393	(+)	0.851	cgggGCGCggggcgc

[a] Matrix name of transcription factor in MatInspector library version 7.1.
[b] Similarity threshold between identified DNA sequence and the matrix of transcription factor binding sequence.
[c] Position of identified DNA sequence from transcriptional start site.
[d] Orientation of identified DNA sequence.
[e] Similarity between the identified DNA sequence and the matrix of transcription factor binding sequence.

element, resulting in the repression of Maf recognition element-dependent gene activation, a feature characteristic of passive repression (61, 62). AP-4 has also been shown to function as a passive repressor by competing with TBP for TATA box binding (4), or by competing with other bHLH transcription factor complexes for E-box binding (63). In the present quantitative proteomic study, TBP remained unchanged. However, two bHLH transcription factors, USF2 and CLOCK, were enriched (Fig. 7, group A), suggesting that they may participate in the regulation of *HDM2* transcription by competing with AP-4 for E-box binding (Fig. 7). It will be of interest to determine whether AP-4 and USF2 or other bHLH transcription factors regulate *HDM2* transcription in a competitive manner.

Other transcription factors, such as CTCF, NFATC2, and SP1, were also significantly enriched in our quantitative proteomic study (Fig. 7, group A). Although the oligonucleotides used in the DNA affinity purification did not contain any binding sequence for these transcription factors, a distal NFAT binding site responsible for *HDM2* transcription repression has been identified (64). In addition, sequence analysis by MatInspector program (39) revealed several putative SP1 and CTCF binding sites distal to the *HDM2*-P2 promoter E-box (Chr. 12, contig NC_000012, 67488540−67489062, 523 bp) (37) (Table II). These observations raise the possibility that regulation of *HDM2* transcription may be coordinated by AP-4 and other transcription factors. For example, distant interaction of AP-4 and SP1 via mutual interaction with GATA-3 was demonstrated to regulate the transcription of the dopamine β-hydroxylase gene (19). It is also noted that a transcriptional repressor ZBTB7A, which is an SP1-interacting protein (65), is also significantly enriched. Our data suggest that AP-4 may

coordinate association of these transcription factors with a repressor molecule(s) to regulate *HDM2* transcription.

II. Active Repression by Direct Recruitment of Repressor Molecules—Transcriptional repression can also be mediated by active repressors, which target chromatin organization via histone deacetylation or methylation (51). For example, MafG, in addition to passive repression, can actively repress target gene expression by recruiting HDAC (66). Similarly, AP-4 has also been reported to repress transcription by recruiting active repressor proteins such as the HDAC complex (Fig. 7, group B), as exemplified by repression of *PAHX-AP1* expression in nonneuronal brain cells (18) and repression of HIV-1 gene expression in T lymphocytes (6). However, our findings suggest that *HDM2* repression by AP-4 occurs via an HDAC-independent mechanism in the colorectal cancer cell line HCT116, indicating that HDAC-independent repression by AP-4 may be tissue-specific. Bimodal repression has been reported for other transcription factors such as SHARP-1 (67) and NRSF (68, 69). Transcriptional repression by NRSF is mediated by an N-terminal domain that recruits HDAC1 and Sin3B (68) or by a C-terminal domain that recruits a corepressor complex consisting of Co-REST and SMARCC2 (69), which belong to the SWI·SNF nucleosome remodeling complex. Interestingly, SMARCC2, as well as four other components of the SWI·SNF complex, were also enriched on the WT *HDM2*-P2 promoter sequence by AP-4 (Fig. 7, group C). Notably, the enrichment ratio of SWI·SNF complex components was higher than that of HDAC complex components (HDAC1, HDAC2, Sin3B, and SAP130). Furthermore, it has been shown that histone H3-Lys-9 methyltransferases, EHMT1 and EHMT2, participate in transcription repression by formation of facultative heterochromatin (51). As shown in

Fig. 7 (group D), EHMT1 and EHMT2, members of the CTBP1 complex, were also enriched on the WT *HDM2*-P2 promoter. Thus, our data suggest that HDAC-independent *HDM2* repression by AP-4 occurs via recruitment of active repressors such as histone methylases or the SWI·SNF complex (Fig. 7).

III. Functional Involvement of AP-4 in DNA Damage Response—Our proteomic study revealed that DNA damage response proteins were the most substantially enriched group of proteins (Fig. 7, group E). Interestingly, a putative UV-responsive region encompassing the AP-4 binding site identified herein has been reported to repress *HDM2* transcription in response to high doses of UV radiation (45, 46). Among the enriched DNA damage-responsive proteins, RAD50 has been demonstrated to participate in the repair of DNA double-strand breaks under the control of BRCA1 (70). RAD50 also interacts with the telomeric-binding protein TERF2 (71), which has been demonstrated to recognize DNA double-strand breaks caused by ionizing radiation (72). Following oxidative or UV-induced DNA damage, APEX1, HMGB1, and PARP2 are the major effectors of DNA base excision repair, whereas BRCA1, PCNA and POLE2 play important roles in nucleotide excision repair (73–76). Thus, AP-4 may also regulate *HDM2* transcription following DNA damage, perhaps by associating with DNA damage-responsive proteins.

Contribution of Q/P-rich Domain to Transcriptional Repression—Incremental truncation of AP-4 revealed that the Q/P-rich domain of AP-4 was, in part, responsible for transcriptional repression. Identification of a Gln/Pro-rich domain repressive activity contrasts with its previously established role in transcription activation (77). Our observations contribute to the increasing body of evidence that Pro- and/or Gln-rich domains mediate transcriptional repression, as exemplified by the Wilms tumor gene *WT1* and Epstein-Barr virus nuclear antigen EBNA3C. The N-terminal P-rich domain of WT1 is shown to interact with the transcriptional corepressor BASP1 (78). Similarly, EBNA3C has a weak transcriptional repression domain enriched with proline and acidic residues that interacts with the corepressor CTBP1 (79). Interestingly, CTBP1 was also enriched in our quantitative proteomics study (Fig. 7, group D). Further studies will be required to determine whether other components in the AP-4 complex interacting with the Gln/Pro-rich domain of AP-4, such as EHMT and CTBP1, mediate the HDAC-independent *HDM2* repression. In addition, our study revealed that several proteins specifically associate with the C-terminal domain of AP-4, such as CTCF, HDAC1, and SP-1. It is also of interest to determine their functional roles contributing to the *HDM2* repression, allowing better understanding of AP-4-mediated HDAC-independent *HDM2* repression.

REFERENCES

1. Hu, Y. F., Lüscher, B., Admon, A., Mermod, N., and Tjian, R. (1990) Transcription factor AP-4 contains multiple dimerization domains that regulate dimer specificity. *Genes Dev.* **4,** 1741–1752
2. Mermod, N., Williams, T. J., and Tjian, R. (1988) Enhancer binding factors AP-4 and AP-1 act in concert to activate SV40 late transcription *in vitro*. *Nature* **332,** 557–561
3. Unk, I., Kiss-Toth, E., and Boros, I. (1994) Transcription factor AP-4 participates in activation of bovine leukemia virus long terminal repeat by p34 tax. *Nucleic Acids Res.* **22,** 4872–4875
4. Ou, S. H., Garcia-Martínez, L. F., Paulssen, E. J., and Gaynor, R. B. (1994) Role of flanking E box motifs in human immunodeficiency virus type 1 TATA element function. *J. Virol.* **68,** 7188–7199
5. Friez, M., Hermansen, R., and Milavetz, B. (1999) Chromatin structure of the simian virus 40 late promoter: a deletional analysis. *J. Virol.* **73,** 1990–1997
6. Imai, K., and Okamoto, T. (2006) Transcriptional repression of human immunodeficiency virus type 1 by AP-4. *J. Biol. Chem.* **281,** 12495–12505
7. Badinga, L., Song, S., Simmen, R. C., and Simmen, F. A. (1998) A distal regulatory region of the insulin-like growth factor binding protein-2 (IGFBP-2) gene interacts with the basic helix-loop-helix transcription factor, AP-4. *Endocrine* **8,** 281–289
8. Comb, M., Mermod, N., Hyman, S. E., Pearlberg, J., Ross, M. E., and Goodman, H. M. (1988) Proteins bound at adjacent DNA elements act synergistically to regulate human proenkephalin cAMP inducible transcription. *EMBO J.* **7,** 3793–3805
9. Fodor, E., Weinrich, S. L., Meister, A., Mermod, N., and Rutter, W. J. (1991) A pancreatic exocrine cell factor and AP4 bind overlapping sites in the amylase 2A enhancer. *Biochemistry* **30,** 8102–8108
10. King-Jones, K., Korge, G., and Lehmann, M. (1999) The helix-loop-helix proteins dAP-4 and Daughterless bind both in vitro and in vivo to SEBP3 sites required for transcriptional activation of the drosophila gene Sgs-4. *J. Mol. Biol.* **291,** 71–82
11. Tsujimoto, K., Ono, T., Sato, M., Nishida, T., Oguma, T., and Tadakuma, T. (2005) Regulation of the expression of caspase-9 by the transcription factor activator protein-4 in glucocorticoid-induced apoptosis. *J. Biol. Chem.* **280,** 27638–27644
12. Jung, P., Menssen, A., Mayr, D., and Hermeking, H. (2008) AP4 encodes a c-MYC-inducible repressor of p21. *Proc. Natl. Acad. Sci. U. S. A.* **105,** 15046–15051
13. Xiu, Y., Nakamura, K., Abe, M., Li, N., Wen, X. S., Jiang, Y., Zhang, D., Tsurui, H., Matsuoka, S., Hamano, Y., Fujii, H., Ono, M., Takai, T., Shimokawa, T., Ra, C., Shirai, T., and Hirose, S. (2002) Transcriptional regulation of Fcgr2b gene by polymorphic promoter region and its contribution to humoral immune responses. *J. Immunol.* **169,** 4340–4346
14. Aranburu, A., Carlsson, R., Persson, C., and Leanderson, T. (2001) Transcription factor AP-4 is a ligand for immunoglobulin-kappa promoter E-box elements. *Biochem. J.* **354,** 431–438
15. Andriamanalijaona, R., Felisaz, N., Kim, S. J., King-Jones, K., Lehmann, M., Pujol, J. P., and Boumediene, K. (2003) Mediation of interleukin-1beta-induced transforming growth factor beta1 expression by activator protein 4 transcription factor in primary cultures of bovine articular chondrocytes: possible cooperation with activator protein 1. *Arthritis Rheum.* **48,** 1569–1581

16. Cui, Y., Narayanan, C. S., Zhou, J., and Kumar, A. (1998) Exon-I is involved in positive as well as negative regulation of human angiotensinogen gene expression. *Gene* **224,** 97–107

17. Littlewood, T. D., and Evan, G. I. (1995) Transcription factors 2: helix-loop-helix. *Protein Profile* **2,** 621–702

18. Kim, M.-Y., Jeong, B. C., Lee, J. H., Kee, H. J., Kook, H., Kim, N. S., Kim, Y. H., Kim, J. K., Ahn, K. Y., and Kim, K. K. (2006) A repressor complex, AP4 transcription factor and geminin, negatively regulates expression of target genes in nonneuronal cells. *Proc. Natl. Acad. Sci. U. S. A.* **103,** 13074–13079

19. Hong, S. J., Choi, H. J., Hong, S., Huh, Y., Chae, H., and Kim, K. S. (2008) Transcription factor GATA-3 regulates the transcriptional activity of dopamine beta-hydroxylase by interacting with Sp1 and AP4. *Neurochem. Res.* **33,** 1821–1831

20. Zhang, and Wang, H. (2000) MDM2 oncogene as a novel target for human cancer therapy. *Curr. Pharm. Des.* **6,** 393–416

21. Haupt, Y., Maya, R., Kazaz, A., and Oren, M. (1997) Mdm2 promotes the rapid degradation of p53. *Nature* **387,** 296–299

22. Kubbutat, M. H., Jones, S. N., and Vousden, K. H. (1997) Regulation of p53 stability by Mdm2. *Nature* **387,** 299–303

23. Wu, X., Bayle, J. H., Olson, D., and Levine, A. J. (1993) The p53-mdm-2 autoregulatory feedback loop. *Genes Dev.* **7,** 1126–1132

24. Zhang, Z., Li, M., Wang, H., Agrawal, S., and Zhang, R. (2003) Antisense therapy targeting MDM2 oncogene in prostate cancer: Effects on proliferation, apoptosis, multiple gene expression, and chemotherapy. *Proc. Natl. Acad. Sci. U. S. A.* **100,** 11636–11641

25. Huang, Q., Raya, A., DeJesus, P., Chao, S. H., Quon, K. C., Caldwell, J. S., Chanda, S. K., Izpisua-Belmonte, J. C., and Schultz, P. G. (2004) Identification of p53 regulators by genome-wide functional analysis. *Proc. Natl. Acad. Sci. U. S. A.* **101,** 3456–3461

26. Gingras, A. C., Aebersold, R., and Raught, B. (2005) Advances in protein complex analysis using mass spectrometry. *J. Physiol.* **563,** 11–21

27. Kerrigan, L. A., and Kadonaga, J. T. (1993) Purification of sequence-specific DNA-binding proteins by affinity chromatography. In *Current Protocols in Molecular Biology* (Ausubel, F. M., Brent, B., Kingston, R. E., Moore, D. D., Seidman, J. G., Smith, J. A., and Struhl, K., eds), pp. 12.10.11–12.10.18, John Wiley and Sons, New York

28. Andrews, N. C., Erdjument-Bromage, H., Davidson, M. B., Tempst, P., and Orkin, S. H. (1993) Erythroid transcription factor NF-E2 is a haematopoietic-specific basic-leucine zipper protein. *Nature* **362,** 722–728

29. Gygi, S. P., Rist, B., Gerber, S. A., Turecek, F., Gelb, M. H., and Aebersold, R. (1999) Quantitative analysis of complex protein mixtures using isotope-coded affinity tags. *Nat. Biotechnol.* **17,** 994–999

30. Ross, P. L., Huang, Y. N., Marchese, J. N., Williamson, B., Parker, K., Hattan, S., Khainovski, N., Pillai, S., Dey, S., Daniels, S., Purkayastha, S., Juhasz, P., Martin, S., Bartlet-Jones, M., He, F., Jacobson, A., and Pappin, D. J. (2004) Multiplexed protein quantitation in *Saccharomyces cerevisiae* using amine-reactive isobaric tagging reagents. *Mol. Cell. Proteomics* **3,** 1154–1169

31. Brand, M., Ranish, J. A., Kummer, N. T., Hamilton, J., Igarashi, K., Francastel, C., Chi, T. H., Crabtree, G. R., Aebersold, R., and Groudine, M. (2004) Dynamic changes in transcription factor complexes during erythroid differentiation revealed by quantitative proteomics. *Nat. Struct. Mol. Biol.* **11,** 73–80

32. Kim, B., Nesvizhskii, A. I., Rani, P. G., Hahn, S., Aebersold, R., and Ranish, J. A. (2007) The transcription elongation factor TFIIS is a component of RNA polymerase II preinitiation complexes. *Proc. Natl. Acad. Sci. U. S. A.* **104,** 16068–16073

33. Ranish, J. A., Yi, E. C., Leslie, D. M., Purvine, S. O., Goodlett, D. R., Eng, J., and Aebersold, R. (2003) The study of macromolecular complexes by quantitative proteomics. *Nat. Genet.* **33,** 349–355

34. Mousson, F., Kolkman, A., Pijnappel, W. W., Timmers, H. T., and Heck, A. J. (2008) Quantitative proteomics reveals regulation of dynamic components within TATA-binding protein (TBP) transcription complexes. *Mol. Cell. Proteomics* **7,** 845–852

35. Himeda, C. L., Ranish, J. A., Angello, J. C., Maire, P., Aebersold, R., and Hauschka, S. D. (2004) Quantitative proteomic identification of Six4 as the trex-binding factor in the muscle creatine kinase enhancer. *Mol. Cell. Biol.* **24,** 2132–2143

36. Himeda, C. L., Ranish, J. A., and Hauschka, S. D. (2008) Quantitative proteomic identification of MAZ as a transcriptional regulator of muscle-specific genes in skeletal and cardiac myocytes. *Mol. Cell. Biol.* **28,** 6521–6535

37. Phelps, M., Darley, M., Primrose, J. N., and Blaydes, J. P. (2003) p53-independent activation of the hdm2-P2 promoter through multiple transcription factor response elements results in elevated hdm2 expression in estrogen receptor alpha-positive breast cancer cells. *Cancer Res.* **63,** 2616–2623

38. Urban, A., Neukirchen, S., and Jaeger, K. E. (1997) A rapid and efficient method for site-directed mutagenesis using one-step overlap extension PCR. *Nucleic Acids Res.* **25,** 2227–2228

39. Cartharius, K., Frech, K., Grote, K., Klocke, B., Haltmeier, M., Klingenhoff, A., Frisch, M., Bayerlein, M., and Werner, T. (2005) MatInspector and beyond: promoter analysis based on transcription factor binding sites. *Bioinformatics* **21,** 2933–2942

40. Chen, Y. R., Juan, H. F., Huang, H. C., Huang, H. H., Lee, Y. J., Liao, M. Y., Tseng, C. W., Lin, L. L., Chen, J. Y., Wang, M. J., Chen, J. H., and Chen, Y. J. (2006) Quantitative proteomic and genomic profiling reveals metastasis-related protein expression patterns in gastric cancer cells. *J. Proteome Res.* **5,** 2727–2742

41. Han, C. L., Chien, C. W., Chen, W. C., Chen, Y. R., Wu, C. P., Li, H., and Chen, Y. J. (2008) A multiplexed quantitative strategy for membrane proteomics: opportunities for mining therapeutic targets for autosomal-dominant polycystic kidney disease. *Mol. Cell. Proteomics* **7,** 1983–1997

42. Li, X. J., Zhang, H., Ranish, J. A., and Aebersold, R. (2003) Automated statistical analysis of protein abundance ratios from data generated by stable-isotope dilution and tandem mass spectrometry. *Anal. Chem.* **75,** 6648–6657

43. Lin, W. T., Hung, W. N., Yian, Y. H., Wu, K. P., Han, C. L., Chen, Y. R., Chen, Y. J., Sung, T. Y., and Hsu, W. L. (2006) Multi-Q: a fully automated tool for multiplexed protein quantitation. *J. Proteome Res.* **5,** 2328–2338

44. Zauberman, A., Flusberg, D., Haupt, Y., Barak, Y., and Oren, M. (1995) A functional p53-responsive intronic promoter is contained within the human mdm2 gene. *Nucleic Acids Res.* **23,** 2584–2592

45. Zeng, X., Keller, D., Wu, L., and Lu, H. (2000) UV but not gamma irradiation accelerates p53-induced apoptosis of teratocarcinoma cells by repressing MDM2 transcription. *Cancer Res.* **60,** 6184–6188

46. Wu, L., and Levine, A. J. (1997) Differential regulation of the p21/WAF-1 and mdm2 genes after high-dose UV irradiation: p53-dependent and p53-independent regulation of the mdm2 gene. *Mol. Med.* **3,** 441–451

47. Bunz, F., Dutriaux, A., Lengauer, C., Waldman, T., Zhou, S., Brown, J. P., Sedivy, J. M., Kinzler, K. W., and Vogelstein, B. (1998) Requirement for p53 and p21 to sustain G2 arrest after DNA damage. *Science* **282,** 1497–1501

48. Wu, W. W., Wang, G., Baek, S. J., and Shen, R. F. (2006) Comparative study of three proteomic quantitative methods, DIGE, cICAT, and iTRAQ, using 2D gel- or LC-MALDI TOF/TOF. *J. Proteome Res.* **5,** 651–658

49. DeSouza, L., Diehl, G., Rodrigues, M. J., Guo, J., Romaschin, A. D., Colgan, T. J., and Siu, K. W. (2005) Search for cancer markers from endometrial tissues using differentially labeled tags iTRAQ and cICAT with multidimensional liquid chromatography and tandem mass spectrometry. *J. Proteome Res.* **4,** 377–386

50. Kim, L. J., Seto, A. G., Nguyen, T. N., and Goodrich, J. A. (2001) Human TAFII130 is a coactivator for NFATp. *Mol. Cell. Biol.* **21,** 3503–3513

51. Thiel, G., Lietz, M., and Hohl, M. (2004) How mammalian transcriptional repressors work. *Eur. J. Biochem.* **271,** 2855–2862

52. Medina, V., Edmonds, B., Young, G. P., James, R., Appleton, S., and Zalewski, P. D. (1997) Induction of caspase-3 protease activity and apoptosis by butyrate and trichostatin A (inhibitors of histone deacetylase): dependence on protein synthesis and synergy with a mitochondrial/cytochrome c-dependent pathway. *Cancer Res.* **57,** 3697–3707

53. Patton, W. F. (2002) Detection technologies in proteome analysis. *J. Chromatogr. B Analyt. Technol. Biomed. Life Sci.* **771,** 3–31

54. Julka, S., and Regnier, F. (2004) Quantification in proteomics through stable isotope coding: a review. *J. Proteome Res.* **3,** 350–363

55. Tan, H. T., Tan, S., Lin, Q., Lim, T. K., Hew, C. L., and Chung, M. C. M. (2008) Quantitative and temporal proteome analysis of butyrate-treated colorectal cancer cells. *Mol. Cell. Proteomics* **7,** 1174–1185

56. Gadgil, H., Jurado, L. A., and Jarrett, H. W. (2001) DNA affinity chromatography of transcription factors. *Anal. Biochem.* **290,** 147–178

57. Righetti, P. G., Castagna, A., Antonioli, P., and Boschetti, E. (2005) Prefractionation techniques in proteome analysis: the mining tools of the

third millennium. *Electrophoresis* **26,** 297–319

58. Yaneva, M., and Tempst, P. (2003) Affinity capture of specific DNA-binding proteins for mass spectrometric identification. *Anal. Chem.* **75,** 6437–6448

59. Petti, F., Thomson, S., and Haley, J. D. (2006) Peptide, domain, and DNA affinity selection in the identification and quantitation of proteins from complex biological samples. *Anal. Biochem.* **356,** 1–11

60. Mittler, G., Butter, F., and Mann, M. (2009) A SILAC-based DNA protein interaction screen that identifies candidate binding proteins to functional DNA elements. *Genome Res.* **19,** 284–293

61. Motohashi, H., Katsuoka, F., Shavit, J. A., Engel, J. D., and Yamamoto, M. (2000) Positive or negative MARE-dependent transcriptional regulation is determined by the abundance of small Maf proteins. *Cell* **103,** 865–875

62. Nagai, T., Igarashi, K., Akasaka, J., Furuyama, K., Fujita, H., Hayashi, N., Yamamoto, M., and Sassa, S. (1998) Regulation of NF-E2 activity in erythroleukemia cell differentiation. *J. Biol. Chem.* **273,** 5358–5365

63. Kim, J. W., Monila, H., Pandey, A., and Lane, M. D. (2007) Upstream stimulatory factors regulate the C/EBPα gene during differentiation of 3T3-L1 preadipocytes. *Biochem. Biophys. Res. Commun.* **354,** 517–521

64. Li, M., Zhang, Z., Hill, D. L., Chen, X., Wang, H., and Zhang, R. (2005) Genistein, a dietary isoflavone, down-regulates the MDM2 oncogene at both transcriptional and posttranslational levels. *Cancer Res.* **65,** 8200–8208

65. Lee, D. K., Suh, D., Edenberg, H. J., and Hur, M. W. (2002) POZ domain transcription factor, FBI-1, represses transcription of ADH5/FDH by interacting with the zinc finger and interfering with DNA binding activity of Sp1. *J. Biol. Chem.* **277,** 26761–26768

66. Motohashi, H., Katsuoka, F., Miyoshi, C., Uchimura, Y., Saitoh, H., Francastel, C., Engel, J. D., and Yamamoto, M. (2006) MafG sumoylation is required for active transcriptional repression. *Mol. Cell. Biol.* **26,** 4652–4663

67. Garriga-Canut, M., Roopra, A., and Buckley, N. J. (2001) The basic helix-loop-helix protein, SHARP-1, represses transcription by a histone deacetylase-dependent and histone deacetylase-independent mechanism. *J. Biol. Chem.* **276,** 14821–14828

68. Naruse, Y., Aoki, T., Kojima, T., and Mori, N. (1999) Neural restrictive silencer factor recruits mSin3 and histone deacetylase complex to repress neuron-specific target genes. *Proc. Natl. Acad. Sci. U. S. A.* **96,** 13691–13696

69. Battaglioli, E., Andrés, M. E., Rose, D. W., Chenoweth, J. G., Rosenfeld, M. G., Anderson, M. E., and Mandel, G. (2002) REST repression of neuronal genes requires components of the hSWI.SNF complex. *J. Biol. Chem.* **277,** 41038–41045

70. Zhong, Q., Chen, C. F., Li, S., Chen, Y., Wang, C. C., Xiao, J., Chen, P. L., Sharp, Z. D., and Lee, W. H. (1999) Association of BRCA1 with the hRad50-hMre11-p95 complex and the DNA damage response. *Science* **285,** 747–750

71. Zhu, X. D., Küster, B., Mann, M., Petrini, J. H., de, and Lange, T. (2000) Cell-cycle-regulated association of RAD50/MRE11/NBS1 with TRF2 and human telomeres. *Nat. Genet.* **25,** 347–352

72. Bradshaw, P. S., Stavropoulos, D. J., and Meyn, M. S. (2005) Human telomeric protein TRF2 associates with genomic double-strand breaks as an early response to DNA damage. *Nat. Genet.* **37,** 193–197

73. Wood, R. D. (1996) DNA repair in eukaryotes. *Annu. Rev. Biochem.* **65,** 135–167

74. Schreiber, V., Amé, J. C., Dollé, P., Schultz, I., Rinaldi, B., Fraulob, V., Ménissier-de Murcia, J., de, and Murcia, G. (2002) Poly(ADP-ribose) polymerase-2 (PARP-2) is required for efficient base excision DNA repair in association with PARP-1 and XRCC1. *J. Biol. Chem.* **277,** 23028–23036

75. Hartman, A. R., and Ford, J. M. (2002) BRCA1 induces DNA damage recognition factors and enhances nucleotide excision repair. *Nat. Genet.* **32,** 180–184

76. Prasad, R., Liu, Y., Deterding, L. J., Poltoratsky, V. P., Kedar, P. S., Horton, J. K., Kanno, S., Asagoshi, K., Hou, E. W., Khodyreva, S. N., Lavrik, O. I., Tomer, K. B., Yasui, A., and Wilson, S. H. (2007) HMGB1 is a cofactor in mammalian base excision repair. *Mol. Cell* **27,** 829–841

77. Choy, B., and Green, M. R. (1993) Eukaryotic activators function during multiple steps of preinitiation complex assembly. *Nature* **366,** 531–536

78. Carpenter, B., Hill, K. J., Charalambous, M., Wagner, K. J., Lahiri, D., James, D. I., Andersen, J. S., Schumacher, V., Royer-Pokora, B., Mann, M., Ward, A., and Roberts, S. G. E. (2004) BASP1 is a transcriptional cosuppressor for the Wilms' tumor suppressor protein WT1. *Mol. Cell. Biol.* **24,** 537–549

79. Touitou, R., Hickabottom, M., Parker, G., Crook, T., and Allday, M. J. (2001) Physical and functional interactions between the corepressor CtBP and the Epstein-Barr virus nuclear antigen EBNA3C. *J. Virol.* **75,** 7749–7755